Activation of Peroxisome Proliferator–Activated Receptor-δ as Novel Therapeutic Strategy to Prevent In-Stent Restenosis and Stent Thrombosis

Jarkko Hytönen,* Olli Leppaenen,* Jan Hinrich Braesen, Wolf-Hagen Schunck, Dominik Mueller, Friedrich Jung, Christoph Mrowietz, Martin Jastroch, Michael von Bergwelt-Baildon, Kai Kappert, Arnd Heuser, Jörg-Detlef Drenckhahn, Burkert Pieske, Ludwig Thierfelder, Seppo Ylä-Herttuala, Florian Blaschke

Objective—Drug-eluting coronary stents reduce restenosis rate and late lumen loss compared with bare-metal stents; however, drug-eluting coronary stents may delay vascular healing and increase late stent thrombosis. The peroxisome proliferator–activated receptor-delta (PPARδ) exhibits actions that could favorably influence outcomes after drug-eluting coronary stents placement.

Approach and Results—Here, we report that PPARδ ligand–coated stents strongly reduce the development of neointima and luminal narrowing in a rabbit model of experimental atherosclerosis. Inhibition of inflammatory gene expression and vascular smooth muscle cell (VSMC) proliferation and migration, prevention of thrombocyte activation and aggregation, and proproliferative effects on endothelial cells were identified as key mechanisms for the prevention of restenosis. Using normal and PPARδ-depleted VSMCs, we show that the observed effects of PPARδ ligand GW0742 on VSMCs and thrombocytes are PPARδ receptor dependent. PPARδ ligand treatment induces expression of pyruvate dehydrogenase kinase isozyme 4 and downregulates the glucose transporter 1 in VSMCs, thus impairing the ability of VSMCs to provide the increased energy demands required for growth factor–stimulated proliferation and migration.

Conclusions—In contrast to commonly used drugs for stent coating, PPARδ ligands not only inhibit inflammatory response and proliferation of VSMCs but also prevent thrombocyte activation and support vessel re-endothelialization. Thus, pharmacological PPARδ activation could be a promising novel strategy to improve drug-eluting coronary stents outcomes. **(*Arterioscler Thromb Vasc Biol*. 2016;36:00-00. DOI: 10.1161/ATVBAHA.115.306962.)**

Key Words: blood platelets ■ coronary restenosis ■ muscle, smooth, vascular ■ peroxisome proliferator-activated receptors ■ stents

Coronary artery disease is the leading cause of mortality and morbidity in industrialized countries.[1] Coronary stents reduce the risk of periprocedural complications and restenosis when compared with angioplasty alone and have revolutionized interventional cardiology; however, in-stent restenosis remains a major clinical obstacle.[2] Drug-eluting stents (DES) have emerged as a highly promising approach to reduce in-stent restenosis. In fact, first-generation DES, such as sirolimus or paclitaxel-eluting stents, and second-generation DES, such as everolimus or zotarolimus-eluting stents, have substantially reduced angiographic and clinical restenosis across broad lesions and patient subsets. Next-generation DES include stents with bioresorbable polymers and bioresorbable stents. However, despite remarkable improvements in stent platform, polymer, and drug, the long-term results of DES usage have been blighted by the dual problems of in-stent restenosis and late stent thrombosis. DES unselectively inhibit migration and proliferation of both vascular smooth muscle cells (VSMCs) and endothelial cells (ECs) and are associated with increased thrombocyte activation and aggregation compared with bare-metal stents.[3–5] In addition, immunosuppressive drugs, such as paclitaxel, decrease numbers and

Received on: December 5, 2015; final version accepted on: May 23, 2016.

From the Department of Molecular Medicine, A.I. Virtanen Institute, University of Eastern Finland, Kuopio, Finland (J.H., S.Y.-H.); Centre for R&D, Uppsala University/County Council of Gaevleborg, Gaevle, Sweden (O.L.); Institute for Pathology, University Clinic of Schleswig-Holstein, Campus Kiel, Kiel, Germany (J.H.B.); Max-Delbrück Center for Molecular Medicine, Berlin, Germany (W.-H.S., D.M., A.H., J.-D.D., L.T., F.B.); Department of Cardiology (B.P., F.B.) and Center for Cardiovascular Research/CCR, Institute of Laboratory Medicine Clinical Chemistry and Pathobiochemistry (K.K.), Charité–Universitaetsmedizin Berlin, Berlin, Germany; Institute of Biomaterial Science and Berlin-Brandenburg Centre for Regenerative Therapies (BCRT), Helmholtz-Zentrum Geesthacht, Teltow, Germany (F.J., C.M.); Institute for Diabetes and Obesity, Helmholtz Zentrum Muenchen, German Research Center for Environmental Health, Germany (M.J.); and Cologne Interventional Immunology, University Hospital of Cologne, Cologne, Germany (M.v.B.-B.).

*These authors contributed equally to this article.

The online-only Data Supplement is available with this article at http://atvb.ahajournals.org/lookup/suppl/doi:10.1161/ATVBAHA.115.306962/-/DC1.

Correspondence to Florian Blaschke, Department of Cardiology, Charité–Universitaetsmedizin Berlin, Campus Virchow-Klinikum, Augustenburger Platz 1, 13353 Berlin, Germany. E-mail florian.blaschke@charite.de

Nonstandard Abbreviations and Acronyms

AMPK	adenosine 5′-monophosphate-activated protein kinase
DES	drug-eluting stent
HUVEC	human umbilical vein endothelial cells
IL-6	interleukin-6
MCP-1	monocyte chemoattractant protein-1
PCI	percutaneous coronary intervention
PDGF	platelet-derived growth factor
PPARδ	peroxisome proliferator–activated receptor-delta
rVSMCs	rat VSMCs
TNFα	tumor necrosis factor-α
VCAM	vascular adhesion molecule
VSMC	vascular smooth muscle cell

proliferative, migratory, adhesive, and tube formation capacities of endothelial progenitor cells, which play an important role in re-endothelialization. Delayed re-endothelialization and impaired endothelial function after DES have been suggested as a cause of increased rates of stent thrombosis compared with bare-metal stents.[6]

The response to percutaneous coronary intervention (PCI)–induced vascular injury is characterized by the sequence of inflammation, granulation, extracellular matrix synthesis, and VSMC proliferation and migration. In this process, VSMCs switch from a quiescent, contractile to a synthetic phenotype that proliferates and migrates in response to chemotactic factors,[7] leading to neointimal thickening and restenosis.[8] PCI-induced vascular injury causes release of growth factors, mainly platelet-derived growth factor (PDGF), which is produced by VSMCs, ECs, platelets, or macrophages and plays an important role in neointima formation.[9] In addition, previous studies have shown that glycolysis is enhanced in response to PDGF and changes in cell metabolism are both a hallmark and requirement for PDGF-induced cell proliferation.[10,11]

The peroxisome proliferator–activated receptor-delta (PPARδ, also called PPARβ), together with the other 2 siblings, PPARα and PPARγ, belongs to the nuclear receptor superfamily of ligand-activated transcription factors. These receptors form heterodimers with retinoid X receptors and bind to consensus response elements in the promoter region of their target genes. In the absence of ligand, PPARδ–retinoid X receptor heterodimers recruit corepressors, silencing transcription by the so-called active repression. Ligand binding induces a conformational change in PPAR–retinoid X receptor complexes, releasing corepressors in exchange for coactivators, which results in increased gene expression.[12] The naturally occurring ligands for PPARδ include polyunsaturated fatty acids, triglycerides, and prostacyclin. In addition, highly potent and selective synthetic PPARδ agonists such as GW501516 or GW0742 have been developed. PPARδ has been associated with regulation of inflammation, cell differentiation, proliferation, and apoptosis.[13] Moreover, PPARδ has beneficial effects on whole-body metabolism and improves several parameters of the metabolic syndrome in defined mouse models.[14] Preclinical and phase I/II trials suggest that PPARδ agonists increase high-density lipoprotein and decrease low-density lipoprotein cholesterol, reduce body fat and improve markers of inflammation in obese subjects.[15,16] These findings prompted us to perform a proof-of-concept study to determine whether PPARδ ligands inhibit in-stent restenosis in a rabbit model of experimental atherosclerosis.

In the present study, we outline a promising role for PPARδ ligand–coated stents to address drawbacks of currently used DES. We demonstrate in vivo that PPARδ ligand–coated stents lead to a significant inhibition of strut-associated neointima when compared with vehicle-coated stents. This effect is mediated by a differential effect on VSMC and EC proliferation and migration, an attenuation of vascular inflammation, and an inhibition of thrombocyte activation and aggregation.

Materials and Methods

Materials and Methods are available in the online-only Data Supplement.

Results

PPARδ Ligand–Coated Stents Inhibit In-Stent Restenosis in Rabbit Atheromatous Arteries

Forty-six methylester conjugated PPARδ ligand (GW0742-Me)– or vehicle (ethanol)–coated stents (21 mm×3.5 mm; Translumina GmbH) were successfully implanted in the aorta of rabbits. A rabbit model of experimental atherosclerosis was used as described in the Method section of this article. To achieve a suitable release kinetic, we modified the synthetic PPARδ ligand GW0742 and produced methylester of GW0742 (GW0742-Me). Pharmacological release kinetic was determined ex vivo and in vivo (Results and Figures II and II in the online-only Data Supplement). Animals were randomized to either high-dose GW0742-Me–coated stents (445.4±61.2 μg), low-dose GW0742-Me–coated stents (151.2±15.4 μg), or vehicle-coated stents (ethanol). Time points for euthanasia were 14 and 42 days after stent deployment (Figure III in the online-only Data Supplement). The rabbits appeared healthy with no signs of drug toxicity identified by weight loss, lethargy, or icterus. We collected blood samples for differential blood count, lipid profile, glucose, C-reactive protein, liver and kidney values at the time of aortic denudation, at the end of the atherogenic diet, before stent placement, and at day 14 and 42 after stent deployment. At all time points, analyzed laboratory values were not significantly different among the groups (Table I in the online-only Data Supplement).

PPARδ ligand–coated stents lead to a significant inhibition of strut-associated neointimal area (29.57% inhibition with high-dose and 46.65% with low-dose–coated stents; $P<0.05$) compared with vehicle (ethanol)–coated stents (Figure 1A and 1C). In addition, cellular proliferation was significantly reduced both in the neointimal area (65.36% inhibition with high-dose and 79.35% with low-dose–coated stents; $P<0.05$) and in the underlying plaque area (53.6% inhibition with high-dose and 74.17% with low-dose–coated stents; $P<0.05$; Figure 1B and 1C). Neointimal smooth muscle cell (41.94% inhibition with high-dose and 53.04% with low-dose–coated stents; $P<0.05$) and macrophage cell

area (40.09% inhibition for high-dose and 71.39% with low-dose–coated stents; $P<0.05$) were significantly decreased with PPARδ ligand–coated stents compared with the control group (Figure 1C). Morphometric analysis of stented rabbit aortas revealed no difference between the groups with respect to external elastic lamina area, stent area, and atherosclerotic plaque area (data not shown).

We next examined inflammatory gene expression in stented and unstented rabbit aortas. PPARδ ligand–coated stents significantly attenuated monocyte chemoattractant protein-1 (MCP-1; 41.66% inhibition with low dose; $P<0.05$) and interleukin-6 (IL-6) mRNA expression (47.3% inhibition with low dose; $P<0.05$) at 42 days after stent placement (Figure 1D, left), whereas no effect on vascular cell adhesion molecule (VCAM) expression was observed (data not shown). In contrast, no difference in gene expression was observed in the arterial wall adjacent to the unstented segments (Figure 1D, right).

PPARδ Activation Inhibits VSMC Proliferation and Migration

VSMC proliferation and migration stimulated by PDGF play a crucial role in the progression of atherosclerosis and the development of restenosis after coronary angioplasty.[17,18] Previous reports suggest that different PPARδ ligands potentiate cell growth, whereas other studies suggest an attenuation of cell growth by PPARδ activation.[19–22] To further analyze the effect of PPARδ activation on VSMC growth, the subtype-specific PPARδ agonist GW0742 was used in rat VSMCs (rVSMCs)

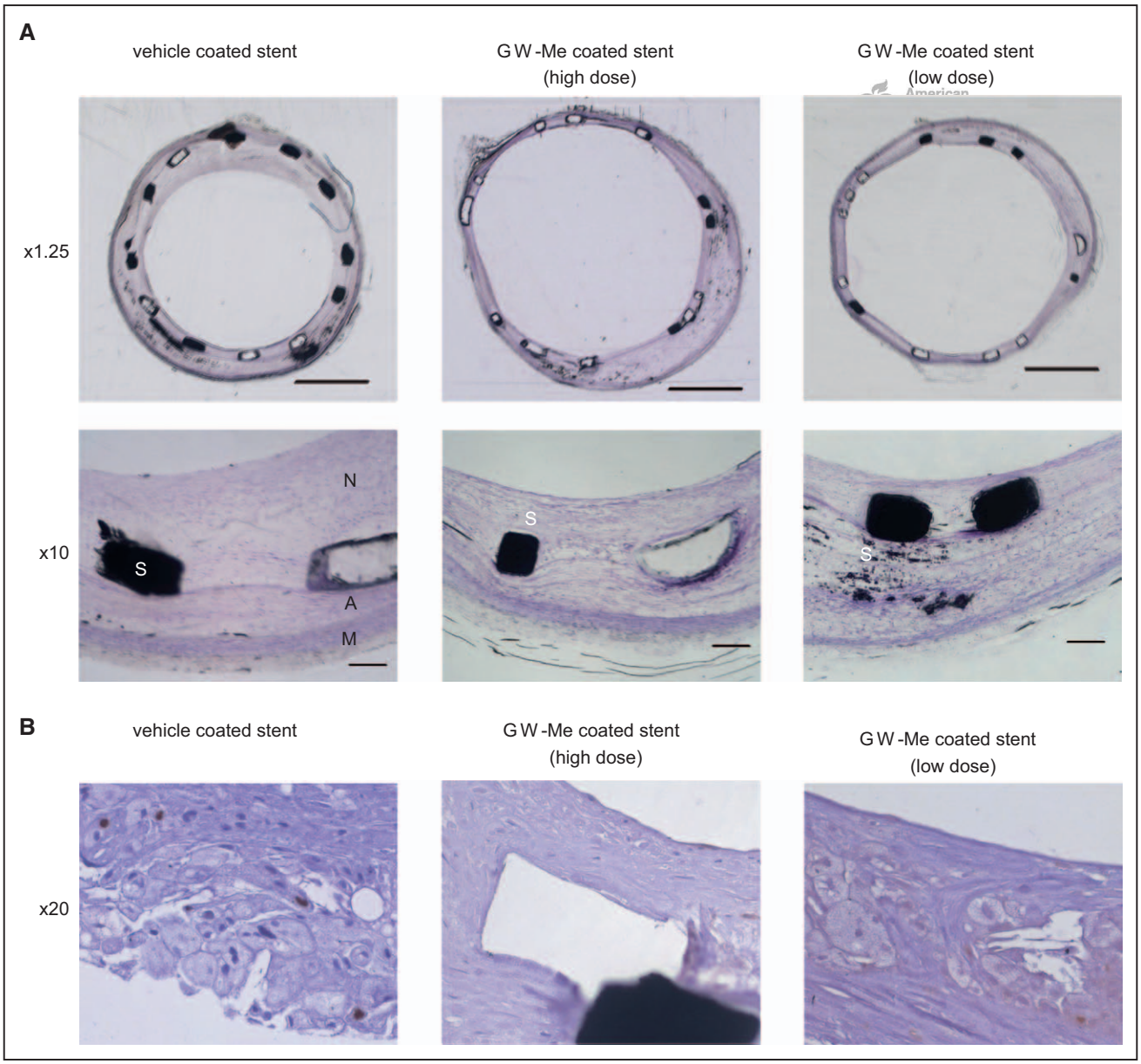

Figure 1. Stents coated with the peroxisome proliferator–activated receptor-delta (PPARδ) ligand GW0742-Me (GW-Me) inhibit in-stent restenosis and inflammatory gene expression in rabbit atheromatous arteries (n=8 per group for 14-d end point, n=10 per group for 42-d end point). Representative cross-sectional histology of the aorta 42 d after implantation of GW0742-Me (low dose and high dose)– or vehicle (EtOH)–coated stents. **A**, Photomicrographs of arterial sections stained with toluidine blue (×1.25 and ×10 magnification). **B**, Arterial sections immunohistochemically stained for KiS1 (×10 magnification). **C**, Histomorphometric analysis of rabbit (*Continued*)

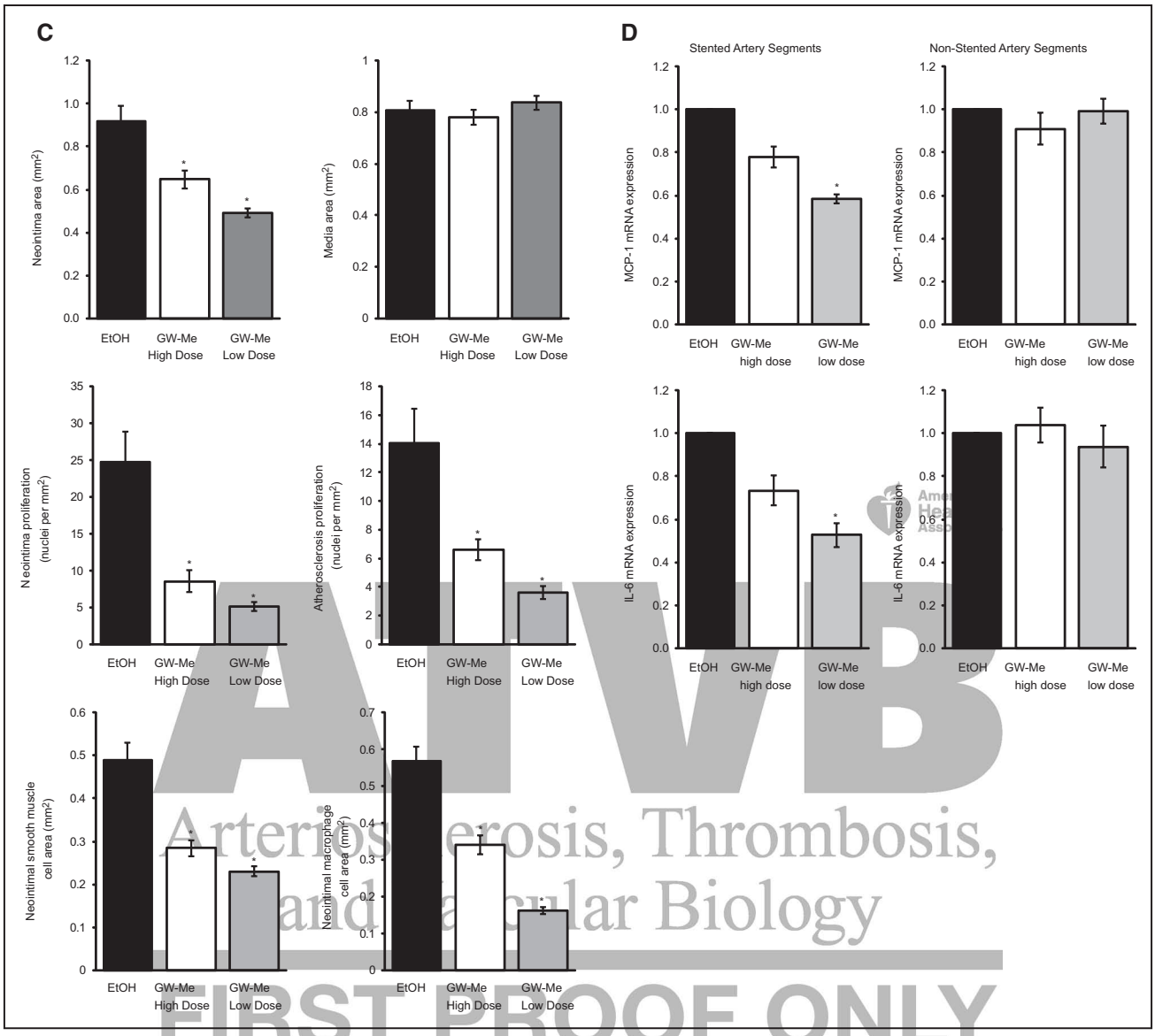

Figure 1 Continued. aortas 42 d after stent deployment. Bar graphs showing reduced neointimal area, attenuated proliferation rate in the neointima and the underlying atherosclerotic lesion, and reduced neointimal vascular smooth muscle cell (VSMC) and macrophage content in vessels implanted with GW0742-Me–coated stents. **D**, Analysis of inflammatory gene expression (monocyte chemoattractant protein [MCP]-1, interleukin [IL]-6) by quantitative real-time polymerase chain reaction in stented (**left**) and nonstented arteries (**right**) artery segments. Results are presented as mean±SEM. **P*<0.05 vs vehicle-coated stents, 1-way ANOVA with post hoc correction (Bonferroni). A indicates atheromatous core; M, media; N, neointima; and S, stent struts.

resuming proliferation by PDGF-BB treatment after G_0/G_1-phase synchronization. GW0742 treatment (Figure 2A, left) inhibited rVSMC proliferation in a dose-dependent manner (40.59% inhibition at 10 µmol/L GW0742; *P*<0.05). To further characterize the role of PPARδ in cell proliferation, VSMCs were isolated from the aorta of PPARδ$^{+/+}$ and PPARδ$^{-/-}$ mice. Electron microscopy analysis of PPARδ$^{-/-}$ VSMCs revealed no morphological differences in size and structure of cell nuclei, mitochondria, endoplasmic reticulum, Golgi complex, and cell–cell contact compared with PPARδ$^{+/+}$ VSMCs (data not shown). Incubation of PPARδ wild-type mouse VSMCs with GW0742 attenuated cell proliferation (32.13% inhibition at 3 µmol/L GW0742; *P*<0.05), whereas no effect was observed in PPARδ-depleted cells (Figure 2A, right).

To analyze individual rVSMC chemotaxis, vehicle-treated (DMSO) or GW0742-treated cells were allowed to migrate in the presence of a PDGF-BB gradient. Cell tracks were recorded by time-lapse microscopy and the Euclidean distance (straight line between starting and end point), the total distance and the directionality of cell migration were determined. As shown in Figure 2B, GW0742 treatment markedly reduced both the Euclidean distance (64.71% inhibition at 3 µmol/L GW0742; *P*<0.05) and the total distance (18.74% inhibition at 3 µmol/L GW0742; *P*<0.05) compared with vehicle-treated cells. Altogether, these data demonstrate that PPARδ ligands inhibit both proliferation and migration of VSMC through a receptor-dependent mechanism.

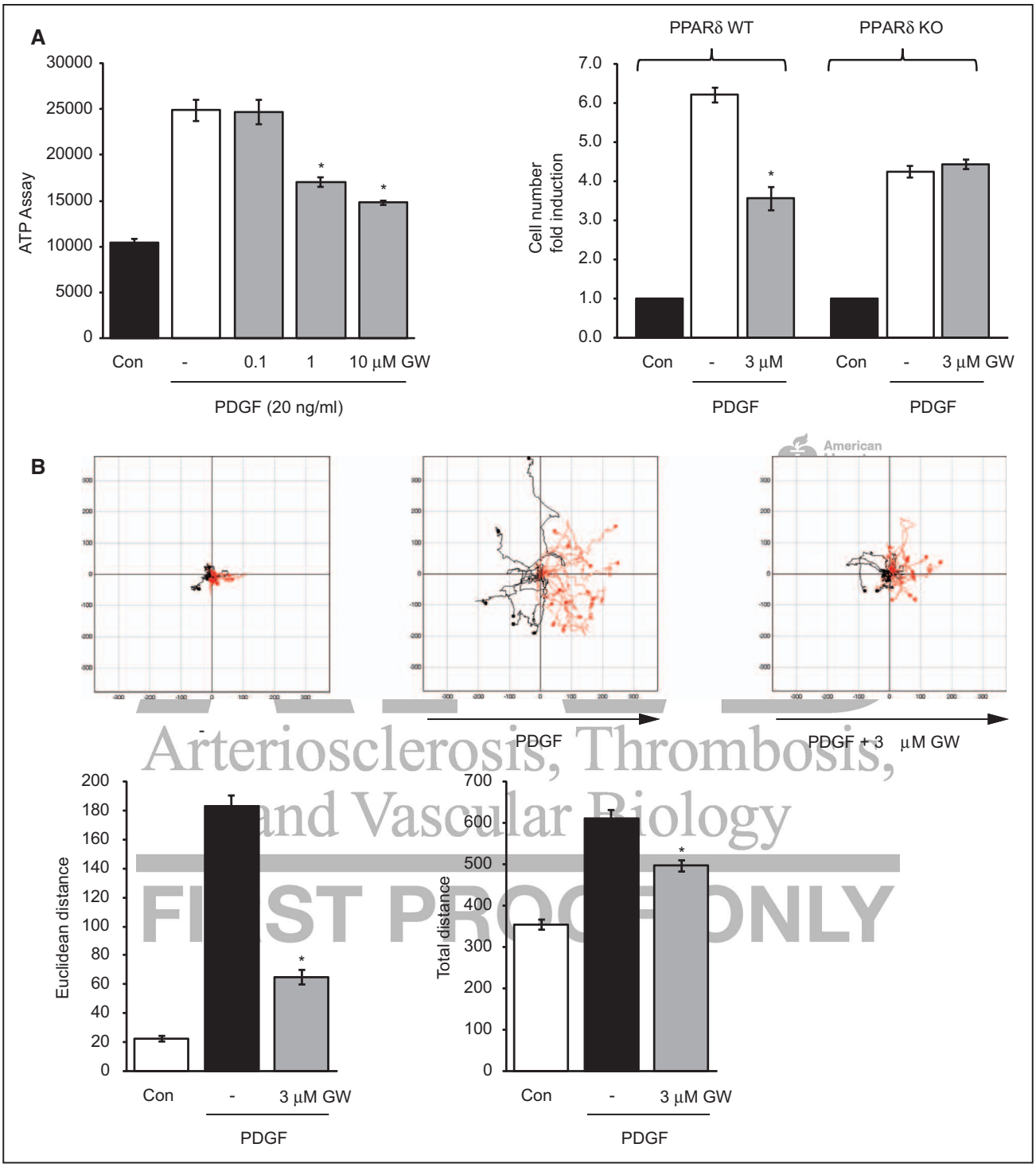

Figure 2. Peroxisome proliferator–activated receptor-delta (PPARδ) activation inhibits growth and platelet-derived growth factor (PDGF)-BB–directed migration of vascular smooth muscle cells (VSMCs). **A**, G_1-arrested rat VSMC (rVSMC) and PPARδ$^{-/-}$ and PPARδ$^{+/+}$ mouse VSMCs (mVSMCs) resumed growth by treatment with PDGF-BB (20 ng/mL). Cells were preincubated with GW0742 (GW) for 24 h as indicated before addition of mitogens. Cell proliferation of rVSMCs was determined using an ATP Assays (**left**). Proliferation of mVSMCs was assayed by counting the cells using a hematocytometer (**right**). **B**, The migration path of 30 representative rVSMC was plotted after normalizing the starting point to x=0 and y=0 (**top**). Red and black lines are cell tracks moving toward the PDGF-BB gradient or moving in other directions, respectively. Diagram shows analysis of euclidean distance and total distance of rVSMCs in the absence of the chemoattractant PDGF-BB (Con), with PDGF-BB alone and in the presence of PDGF-BB and GW0742. Data are presented as mean±SEM. *P<0.05 vs PDGF-stimulated cells, 1-way ANOVA with post hoc correction (Bonferroni).

Because VCMC proliferation and migration is associated with higher energy requirements, we examined the effect of GW0742 on both glycolytic flux (extracellular acidification rate) and mitochondrial oxygen consumption (oxygen consumption rate) using extracellular flux technology. rVSMCs were incubated with 10 μmol/L GW074 or vehicle for 24

hours and changes in glycolysis in response to both acute (data not shown) and chronic PDGF-BB (24 hours) treatment were analyzed. As depicted in Figure 3A (left), PDGF addition increased extracellular acidification rate (3.93-fold versus unstimulated cells; $P<0.05$), which was significantly reduced in GW0742 pretreated rVSMCs (24.32% inhibition; $P<0.05$). Oligomycin was used to eliminate mitochondrial ATP production, thus inducing maximal glycolytic response. GW0742 (Figure 3A, right) significantly attenuated oligomycin-induced increase in glycolysis (24.42% inhibition; $P<0.05$). Next, the effect of GW0742 on mitochondrial oxygen consumption in both acute (data not shown) and chronic PDGF-BB–treated rVSMCs was analyzed. Treatment with GW0742 significantly decreased the maximal respiratory capacity without PDGF-BB (32.34% inhibition; $P<0.05$; Figure 3B, left). ATP-linked respiration was maintained during PDGF-BB treatment and compromised by GW0742 in the absence of PDGF-BB (ATP-linked respiration: basal minus oligomycin [proton leak] respiration; 23.03% inhibition; $P<0.05$; Figure 3C). As GW0742 increased mitochondrial proton leak respiration (measured after oligomycin addition; Figure 3B, center), the reserve respiratory capacity was almost abolished on GW0742 treatment without PDGF-BB (Figure 3B, right) to maintain ATP production. Taken together oxidative phosphorylation and glycolysis, PDGF enhances energy metabolism by increasing glycolysis and shifting ATP production

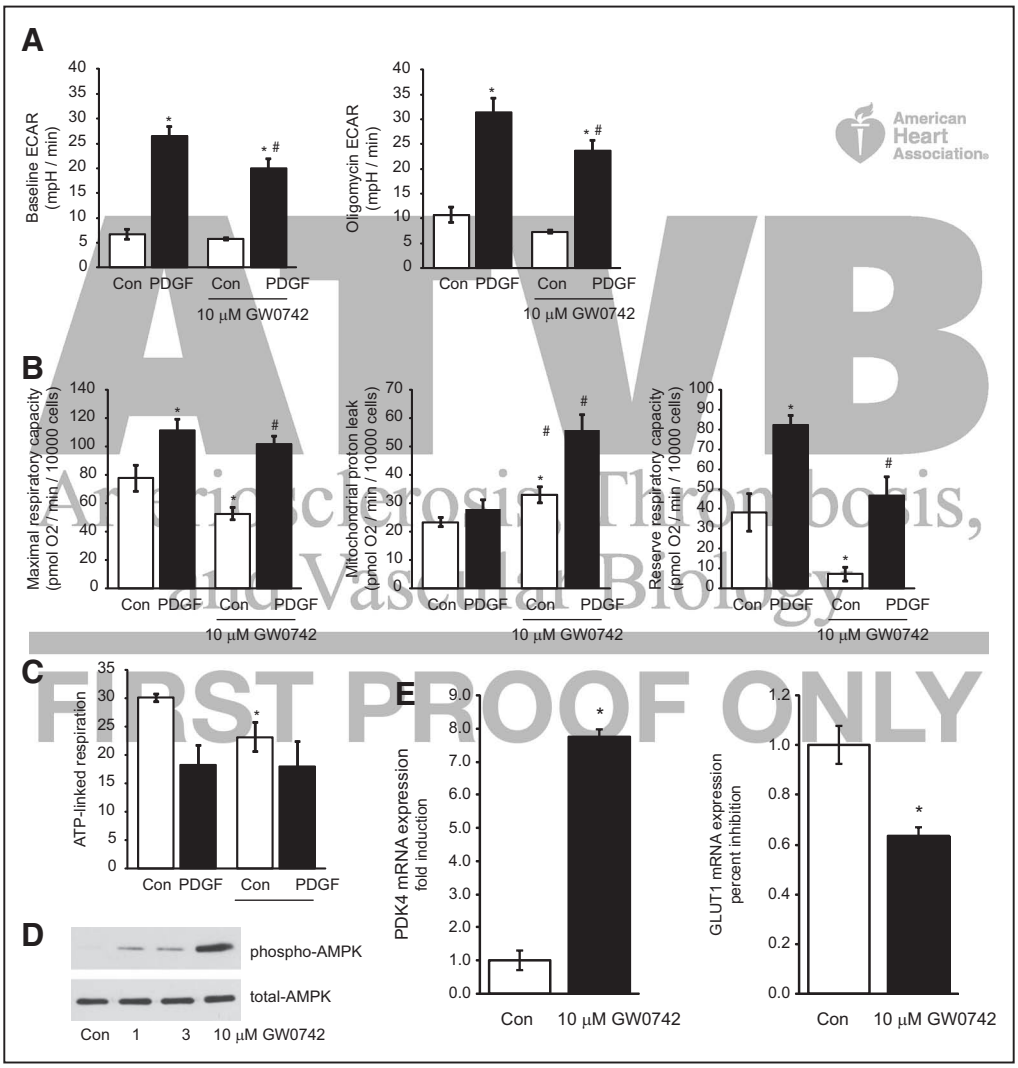

Figure 3. Peroxisome proliferator–activated receptor-delta (PPARδ) activation attenuates glycolytic flux and mitochondrial respiration. **A**, PPARδ activation attenuates platelet-derived growth factor (PDGF)–induced (**left**) and oligomycin-induced (**right**) increase of extracellular acidification rate (ECAR). Rat VSMCs (rVSMC), incubated with 10 μmol/L GW0742 or vehicle (DMSO), were stimulated with or without platelet-derived growth factor (PDGF)-BB (25 ng/mL) for 24 h, and ECAR was measured over time. Oligomycin (2 μg/mL) was injected to determine the glycolytic response to inhibition of mitochondrial ATP synthesis. **B**, PPARδ activation reduces the maximal reserve capacity (**left**), protone leak (**middle**), and mitochondrial reserve capacity (**right**) in unstimulated and PDGF-treated rVSMCs. **C**, PPARδ activation decreases the coupling efficiency in unstimulated and PDGF-treated rVSMCs. The measurements were normalized to the total cell number determined by DAPI staining. **D**, PPARδ activation induces adenosine 5′-monophosphate-activated protein kinase (AMPK) phosphorylation in rVSMCs. **E**, rVSMCs were treated with vehicle (DMSO) or PPARδ ligand GW0742 (10 μmol/L) for 24 h. Total RNA was isolated and pyruvate dehydrogenase kinase isozyme 4 (PDK4) and Glut1 mRNA was measured by quantitative real-time polymerase chain reaction (PCR). Results are presented as mean±SEM. *$P<0.05$ compared with control; #$P<0.05$ compared with PDGF-BB, 1-way ANOVA with post hoc correction (Bonferroni).

toward glycolysis (Warburg-like effect). GW0742 attenuates glycolytic pathways and reduces the metabolic scope of mitochondria by decreasing spare respiratory capacity.

The adenosine 5′-monophosphate-activated protein kinase (AMPK) is a key metabolic sensor that responds to cellular energy deprivation by inhibiting ATP-depleting processes and ATP-promoting processes that increase ATP synthesis within the cell.[23] This prompted us to investigate whether PPARδ ligands induce AMPK phosphorylation. As shown in Figure 3D, stimulation of rVSMCs with GW0742 dose-dependently induced AMPK phosphorylation at threonine 172.

To further characterize the role of PPARδ in energy metabolism, rVSMCs were stimulated with GW0742 and metabolic gene regulation was analyzed. As shown in Figure 3E, PPARδ ligand treatment induces expression of pyruvate dehydrogenase kinase isozyme 4 mRNA (7.74-fold versus unstimulated cells; $P<0.05$), whereas the expression of key regulators of fatty acid transport (Fabp3) and oxidation (Cpt1b, SCD1, SCD2, Acsl1, and Acot1) were unaltered by GW0742 treatment (data not shown). In contrast, the expression of GLUT1, the predominant glucose transporter protein in VSMCs,[24] was markedly downregulated (36.0% inhibition; $P<0.05$).

PPARδ Activation Suppresses Cytokine-Induced Inflammatory Gene Expression in VSMCs

Because inflammation is a key component in in-stent restenotic lesion formation,[25] we analyzed the function of PPARδ in VSMCs in this process. To determine the effect of synthetic PPARδ ligands on cytokine-induced inflammatory gene expression, quiescent rVSMCs, pretreated with GW0742 for 24 hours, were stimulated with tumor necrosis factor-α (10 ng/mL) for additional 8 hours. As depicted in Figure 4A, PPARδ ligand inhibits tumor necrosis factor-α–stimulated IL-6, MCP-1, and VCAM mRNA expression in a dose-dependent manner (at 10 μmol/L GW0742 64.69% inhibition of IL-6; 69.0% inhibition of MCP-1; 75.83% inhibition of VCAM versus tumor necrosis factor-α alone; $P<0.05$). We next used mouse VSMCs isolated from the aorta of PPARδ$^{+/+}$ and PPARδ$^{-/-}$ mice to further address whether the observed inhibitory effect is mediated by PPARδ. The inhibitory effect of GW0742 (Figure 4B) on inflammatory gene expression in PPARδ wild-type mouse VSMCs was completely abolished in PPARδ knockout cells, demonstrating that PPARδ ligands repress IL-6, MCP-1, and VCAM through a receptor-dependent mechanism.

Previous studies indicate that, in the absence of a specific ligand, PPARδ binds the transcriptional repressor B-cell lymphoma 6 (Bcl-6) and PPARδ ligand binding causes a dissociation of Bcl-6 from PPARδ.[26] This interaction prompted us to address the role of Bcl-6 in regulating inflammatory gene expression in VSMCs. Therefore, we transiently transfected rVSMCs with a Bcl-6 overexpression vector. As shown in Figure 4C, Bcl-6 overexpression resulted in a significant inhibition of IL-6, MCP-1, and VCAM mRNA expression in rVSMCs. We next performed chromatin immunoprecipitation assays to determine whether PPARδ ligand treatment induces Bcl-6 binding to the endogenous IL-6, MCP-1, and VCAM promoter. Using primer pairs that cover regions in the proximal IL-6, MCP-1, or VCAM promoter, we demonstrate that PPARδ ligand treatment induces Bcl-6 binding to the corresponding inflammatory gene promoter sequences (Figure 4D). Together, these data show that PPARδ ligand treatment of VSMCs induces a dissociation of Bcl-6 from PPARδ and subsequent binding to specific regions within inflammatory gene promoters, thus inhibiting corresponding gene expression.

PPARδ Ligand Inhibits Thrombocyte Activation and Aggregation

Platelets not only are essential to hemostasis and thrombosis but also activate immune cells and mediate inflammation.[27] Although platelets contain no nucleus, many nuclear receptors were found to be expressed in platelets including all 3 PPAR subtypes and their binding partner retinoid X receptor.[28–30] Thus, we investigated the effect of PPARδ ligand on thrombocyte activation and aggregation in vitro. Consistent with the previous observation,[29] PPARδ was expressed in human platelets (Figure 5A). PPARδ ligand GW0742 dose-dependently inhibited ristocetin (0.75 μg/mL)–induced maximal aggregation (56.13% inhibition at 100 μmol/L GW0742) and maximal aggregation velocity (55.77% inhibition at 100 μmol/L GW0742) of human platelets in vitro. However, GW0742 did not affect collagen-induced platelet aggregation (data not shown).

We next performed activation assays in platelets isolated from PPARδ$^{-/-}$ and age-matched controls. Notably, GW0742 significantly attenuated ADP-induced thrombocyte aggregation in PPARδ$^{+/+}$ platelets (28.38% inhibition at 10 μmol/L GW0742), whereas no effect was observed in PPARδ-depleted platelets (Figure 5B). Interestingly, ADP-induced thrombocyte aggregation was attenuated in PPARδ knockout compared with wild-type platelets.

To investigate the effect of PPARδ ligand–coated stents on thrombocyte activation and aggregation, GW0742-Me– and vehicle (ethanol)–coated stents were implanted in a low-grade thrombogenic closed-loop system and perfused with human platelet-rich plasma at shear rates far below the threshold value at which activation of platelets occurs.[31] Number of circulating platelets, glycoprotein (GP) Ib and IIb/IIIa expression and activation (PAC-1 binding), P-selectin (CD62) and CD63 expression were evaluated before and after 1, 11, and 21 circulations (Figure 5D). The number of single circulating platelets was significantly reduced by 15.2% after 21 circulations ($P<0.05$) of vehicle-coated stents, whereas no effect on platelet number was observed with PPARδ ligand–coated stents. In contrast to GW0742-Me–coated stents, the platelet reactivity index increased after perfusion of vehicle-coated stents by 12.3% ($P<0.05$), indicating that the decrease in circulating platelets is attributable to an increased adherence to the stent, rather than to aggregate formation. In accordance, platelet thrombi were observed between struts of vehicle-coated stents (Figure 5C), but not between struts of GW0742-Me–coated stents. As determined by flow cytometry, the density of GP Ib receptor per platelet was significantly reduced in the vehicle-coated stent group (–12.4%; $P<0.05$) but remained unchanged in the GW0742-Me–coated stent group. After 21 circulations, the density of GP IIb/IIIa and the number of PAC-1–positive

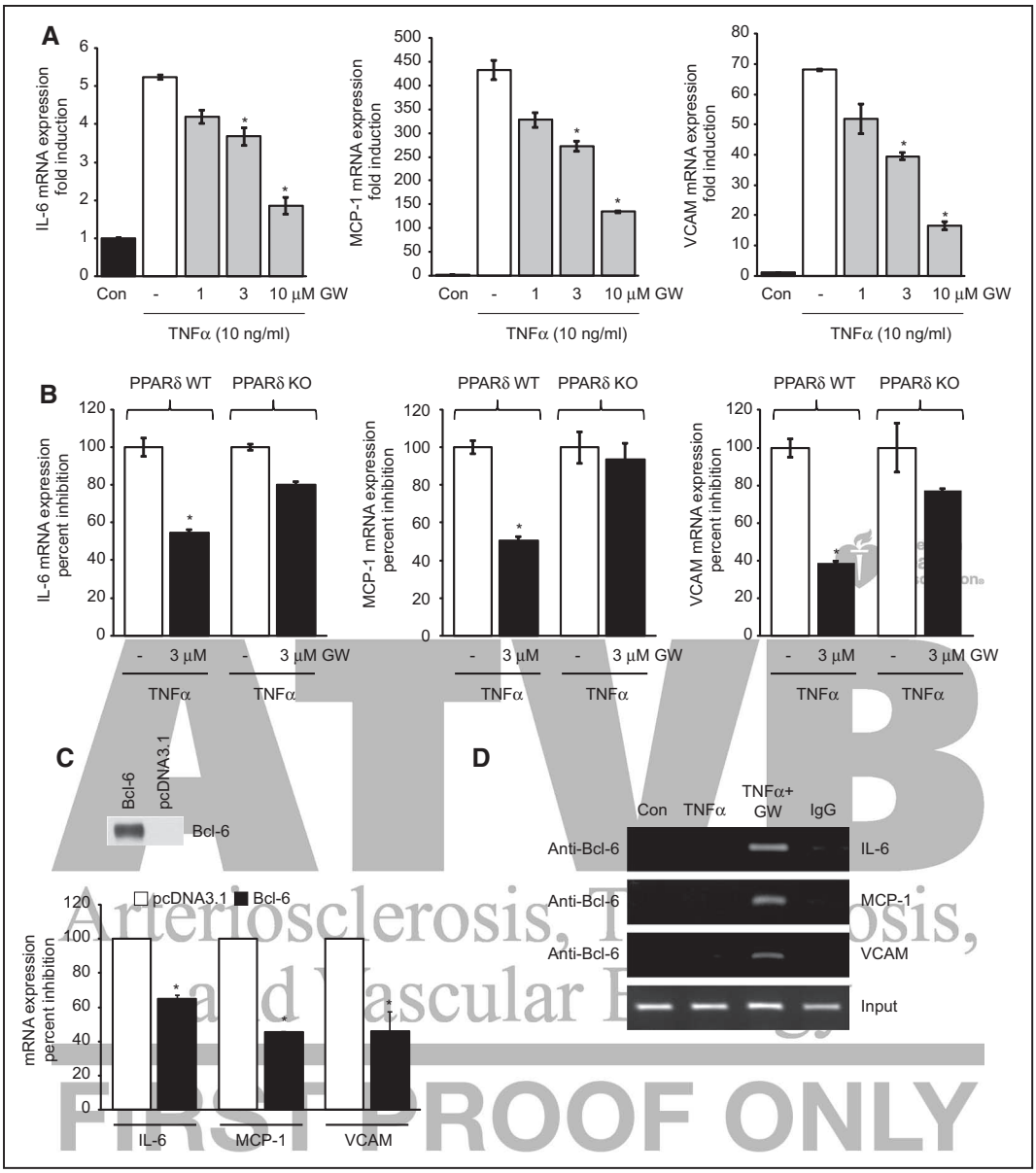

Figure 4. Peroxisome proliferator–activated receptor-delta (PPARδ) activation inhibits tumor necrosis factor (TNF)-α–induced inflammatory gene expression in G_1-arrested rat vascular smooth muscle cell (rVSMC) (**A**) and PPARδ$^{+/+}$ mouse VSMCs (**B**). Serum-deprived cells were pretreated with vehicle (DMSO) or the indicated concentrations of PPARδ ligand GW0742 (GW) for 24 h, followed by stimulation with TNFα (10 ng/mL). Total RNA was isolated and interleukin (IL)-6, monocyte chemoattractant protein (MCP)-1, and VCAM mRNA expression was measured by quantitative real-time polymerase chain reaction (PCR). **C**, Overexpression of Bcl-6 attenuates IL-6, MCP-1, and VCAM mRNA expression in rVSMCs. Cells were transiently transfected with a Bcl-6 expression vector or an empty control vector (pcDNA3.1). At 24 h after transfection, cells were serum starved followed by TNFα (10 ng/mL) stimulation. Total RNA was isolated, and IL-6, MCP-1, and VCAM expressions were analyzed by quantitative real-time RT-PCR. **D**, PPARδ ligands induce Bcl-6 binding to the IL-6, MCP-1, and VCAM promoter. Chromatin immunoprecipitation assays were performed on chromatin isolated from serum-deprived rVSMCs treated with vehicle (DMSO) or GW0742 (10 μmol/L) and stimulated with TNFα (10 ng/mL). All experiments were repeated at least 3 times with different cell preparations of primary VSMCs. Data are expressed as fold induction±SEM over unstimulated control (Con). **P*<0.05 vs TNFα-treated cells, 1-way ANOVA with post hoc correction (Bonferroni) or Student *t* test, as appropriate. KO indicates knockout; and WT, wild-type.

platelets were increased with vehicle-coated stents by 13% and 6.9% (both $P<0.05$), indicating thrombocyte activation. In contrast, in GW0742-Me–coated stents, no changes in the expression of GP IIb/IIIa and PAC-1 on the platelet surface was observed. Finally, the concentration of the thrombin–antithrombin III complex, indicating an activation of the coagulation system, was significantly increased in the vehicle-coated group after 21 circulations (+37.9%; $P<0.05$), but remained unchanged in the GW0742-Me–coated group (data not shown). The fraction of CD62- and CD63-positive platelets did not differ among the groups (data not shown).

PPARδ Activation Induces Human Umbilical Vein Endothelial Cell Proliferation and Migration

PPARδ regulates EC proliferation, angiogenesis, and EC survival.[32] However, the role of PPARδ in ECs is controversial, as

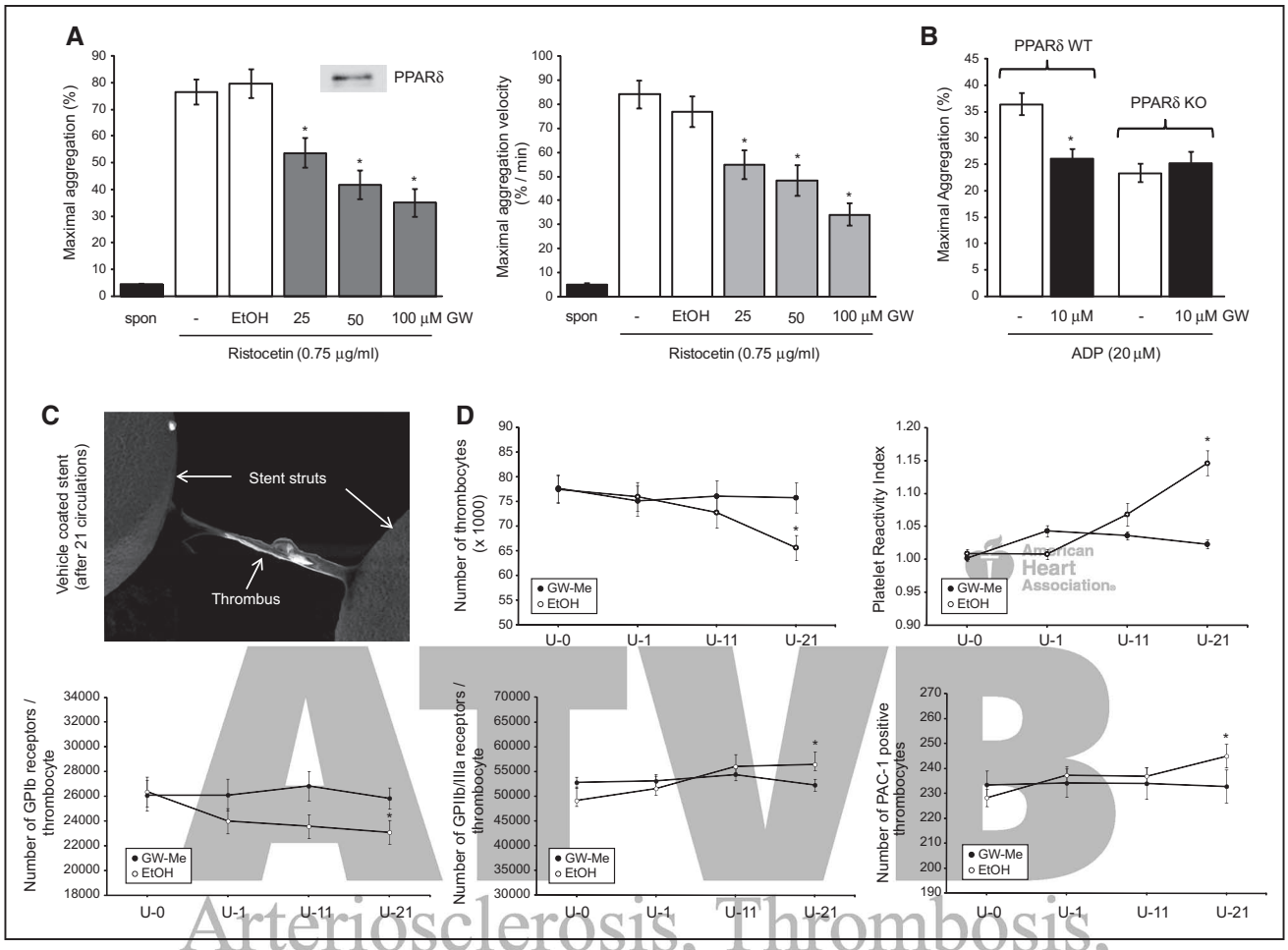

Figure 5. Peroxisome proliferator–activated receptor-delta (PPARδ) activation inhibits thrombocyte activation and aggregation. **A**, PPARδ ligand GW0742 (GW) inhibits ristocetin-induced maximal aggregation (**left**) and maximal aggregation velocity (**right**) of human platelets. Human platelet-rich plasma was incubated with GW0742 for 5 min as indicated, followed by stimulation with ristocetin (0.75 µg/mL). Western blot showing PPARδ protein expression (**top**). **B**, PPARδ$^{-/-}$ and PPARδ$^{+/+}$ mouse platelets were pretreated with GW0742 (10 µmol/L) for 5 min, followed by stimulation with ADP (10 µmol/L). **C** and **D**, PPARδ ligand GW0742-Me (GW-Me)– and vehicle-coated stents (n=6 per group) were implanted in a closed-loop system and perfused with human platelet-rich plasma. Raster electron microscopy reveals formation of thrombi between vehicle (EtOH)–coated stent struts after 21 circulations (**C**). Thrombocyte activation and aggregation was measured immediately after filling of the perfusion system (U-0) and after 1, 11, and 21 circulations (U-0, U-1, U-11, and U-21) (**D**). Results are presented as mean±SEM. **P*<0.05 vs ristocetin or ADP-stimulated platelets, 1-way ANOVA with post hoc correction (Bonferroni) or Student *t* test, as appropriate. KO indicates knockout; and WT, wild-type.

both an inhibition and induction of EC proliferation and angiogenesis on PPARδ ligand stimulation has been reported.[33,34]

Treatment of primary human umbilical vein endothelial cells (HUVECs) with PPARδ ligand (1 µmol/L GW0742) increased EC number (1.17-fold versus unstimulated control), whereas both sirolimus and tacrolimus attenuated HUVEC proliferation compared with untreated control cells (24.09% inhibition at 10 nmol/L sirolimus (36.42% inhibition at 20 µmol/L tacrolimus; $P<0.05$; Figure 6A). To analyze chemotaxis of HUVECs, vehicle-treated (DMSO) or GW0742-treated cells were allowed to migrate in the presence of a VEGF gradient. Cell tracks were recorded by time-lapse microscopy, and the Euclidean distance and total distance were analyzed. GW0742 treatment significantly enhanced the chemotaxis of HUVECs compared with vehicle-treated cells (Figure 6B). To analyze the effect of PPARδ ligands on cell attachment and spreading dynamics, we used the xCELLigence System. As shown in Figure 6C, GW0742 increased adhesion and spreading of HUVECs when compared with untreated cells.

Vascular Injury Induces PPARδ Expression in Rat Carotid Arteries and Human Coronary Arteries

As shown in Figure 7A, PPARδ expression was upregulated in the neointima 14 days after carotid artery balloon injury in 3-month-old Sprague–Dawley rats. Similar to the rat carotid artery injury model, we observed increased PPARδ expression in human coronary arteries after PCI. At 2 weeks after stenting, the stent struts were covered by neointimal tissue, composed mainly of VSMCs with infiltrating macrophages. At this time point, PPARδ expression was highly upregulated in the neointima in both macrophages and VSMCs compared with the underlying atherosclerotic lesion. In contrast, 2 days after PCI without stent placement and 3 years after stenting, only weak PPARδ expression was detected in the atherosclerotic lesions and neointimal areas (Figure 7B and 7C).

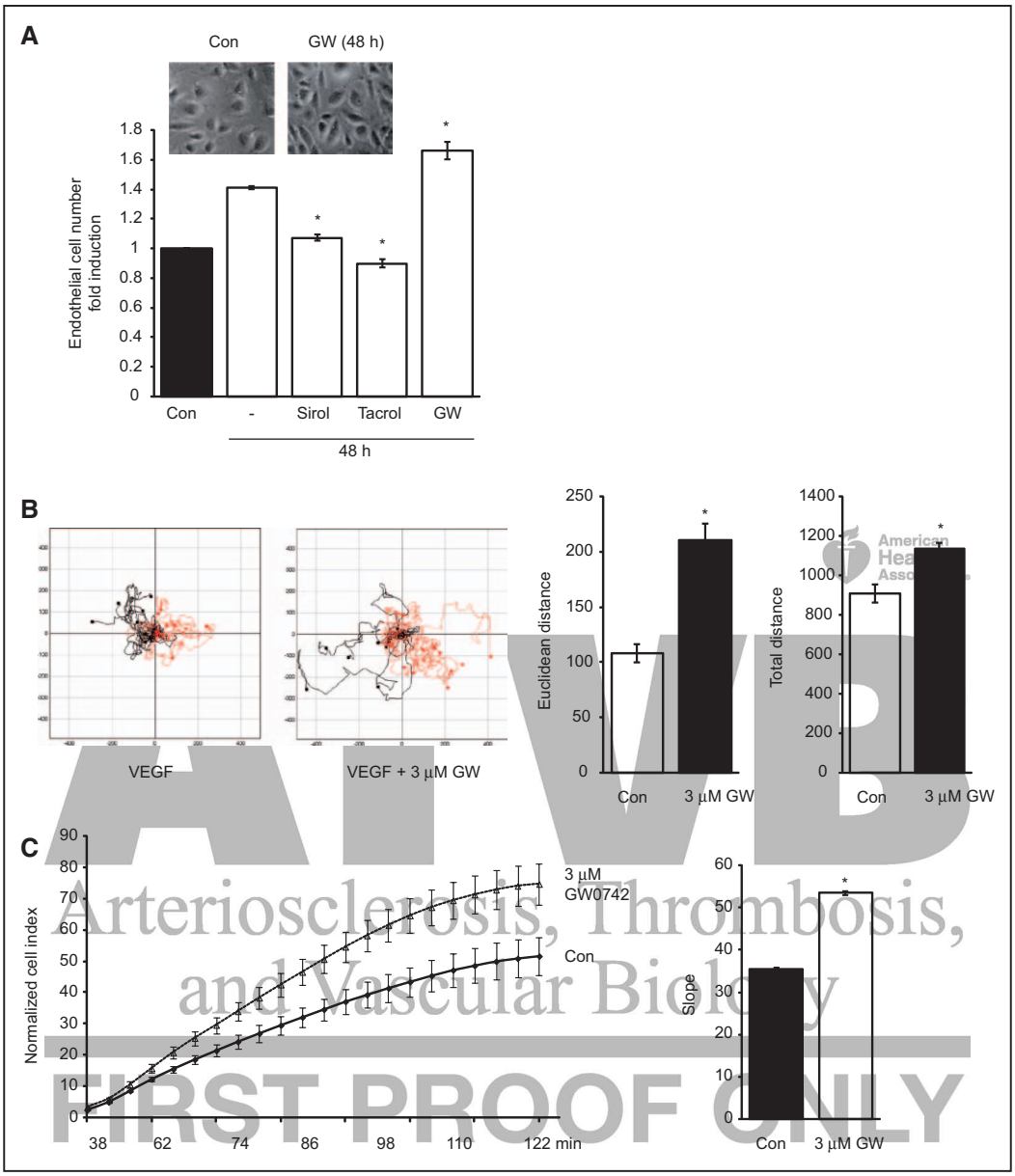

Figure 6. A, Peroxisome proliferator–activated receptor-delta (PPARδ) ligand GW0742 (GW) induces proliferation of human umbilical vein endothelial cells (HUVECs) in vitro. Sirolimus (10 nmol/L), tacrolimus (20 μmol/L), or GW0742 (1 μmol/L) were added in normal growth medium. After 48 h, cell numbers were quantified using a confocal laser microscope. **B**, PPARδ ligand GW0742 (3 μmol/L) increases migration of HUVECs. The migration path of 30 representative HUVECs was plotted after normalizing the starting point to x=0 and y=0. Diagram shows analysis of euclidean distance and total distance of HUVECs in the presence or absence of GW0742. **C**, PPARδ ligand GW0742 increases adhesion and spreading of HUVECs. Cells (10 000 per well) were plated on a 96-well xCELLigence microtiter plate (E-plate), and change in cell index was measured using the xCELLigence impedance system. Results are presented as mean±SEM. *P<0.05 vs untreated cells, 1-way ANOVA with post hoc correction (Bonferroni) or Student t test, as appropriate.

Discussion

We demonstrate that PPARδ ligand–coated stents strongly reduce neointima formation in a rabbit model of experimental atherosclerosis. We attribute this effect to an inhibition of VSMC proliferation, reduced migration, and downregulated inflammatory gene expression. Furthermore, we observed an attenuation of thrombocyte activation and aggregation, as well as an induction of EC adhesion, proliferation, and chemotaxis according to the mechanistic schema that we suggest (Figure VI in the online-only Data Supplement).

The neointima in our rabbit model of experimental atherosclerosis closely mimicked the angioplasty processes in humans, as stents are implanted in preformed atherosclerotic lesions. Aside from stent design, the rate and duration of drug release from the stent and the accumulation of drug in the vessel wall plays an important role in arterial healing.[35] As high-performance liquid chromatography–based analysis depicted an ≈100% GW0742 release from coated stents in vitro within 15 minutes, we modified the solubility of GW074 by methylester conjugation. Using GW0742-Me–coated stents, we achieved a sustained drug release and

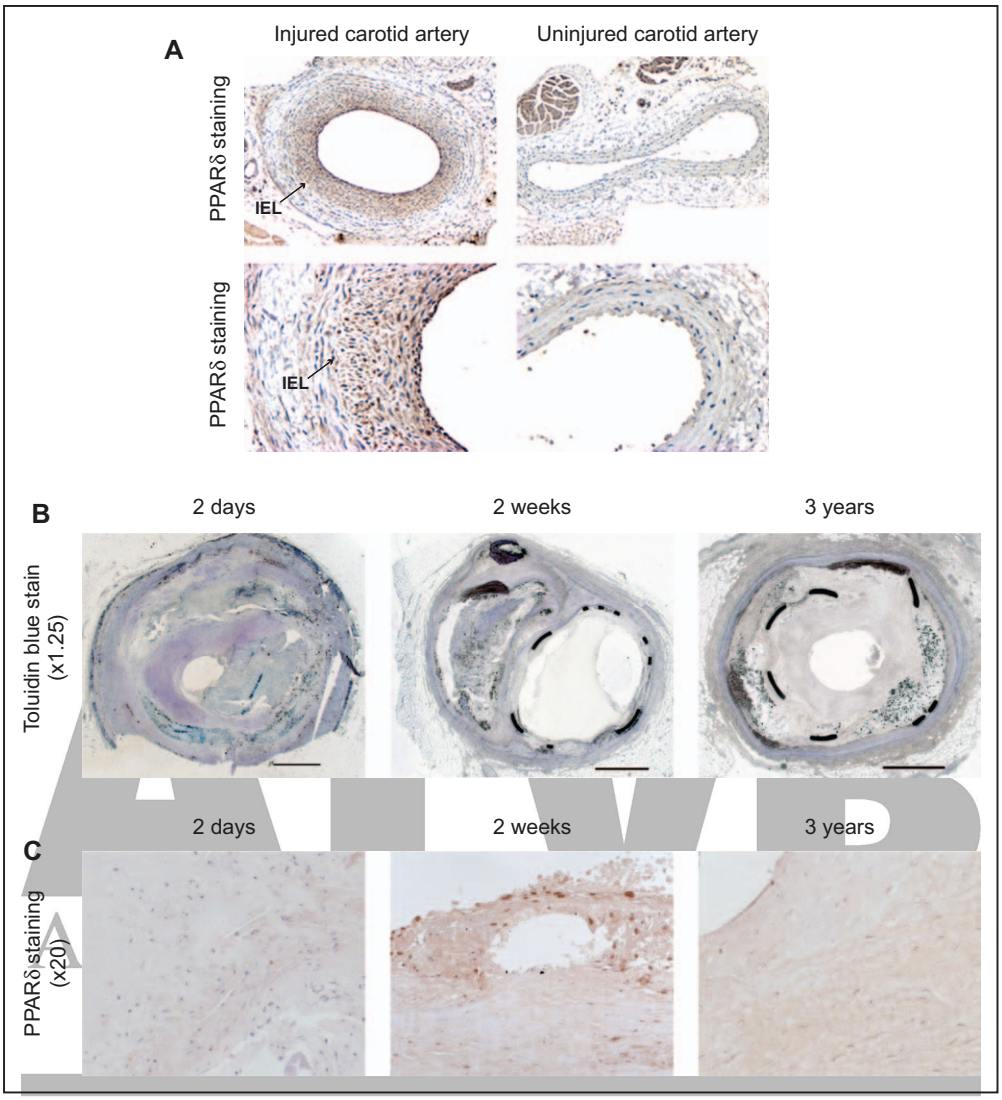

Figure 7. Peroxisome proliferator–activated receptor-delta (PPARδ) expression is highly upregulated in rat and human neointima. **A**, Representative photomicrographs of histological cross sections of balloon-injured rat carotid arteries demonstrate strong PPARδ immunoreactivity in the neointima with weak staining in the media 2 wk after injury (n=8 per group). Arrows indicate the internal elastic lamina (IEL). **B** and **C**, Serial sections of a human nonstented left anterior descending coronary artery 2 d after PTCA (no stent; **left**), a left anterior descending coronary artery 2 wk after stenting (**middle**) and a left circumflex coronary artery 3 y after stenting (**right**). **B**, Toluidine blue staining (×1.25 magnification) of the specimens depict a thrombus (**left**) and early (**middle**) and late in-stent restenosis (**right**). **C**, PPARδ (×20 magnification, brown staining) expression is highly upregulated in the neointima 2 wk after stenting.

intramural deposition both in vitro and in vivo. We show that GW0742-Me–coated stents markedly reduce neointima formation and luminal narrowing both 14 and 42 days after stent placement. This result was accompanied by a significant reduction in cell proliferation both in the neointima and in the underlying atherosclerotic lesion. In addition, stent coating with GW0742-Me strongly attenuates inflammatory gene expression in the underlying vessel wall. However, a limitation of our study is the lack of a comparison with a commercially available DES. We also analyzed thrombocyte deposition 14 days after stent placement (data not shown). However, thrombocyte deposition to uncovered stent struts 14 days after placement of vehicle or GW0742-Me–coated stents was rare, as adhesion of platelets to the endoluminal side of the stents occurs early after stent deployment.[36] Interestingly, whereas our in vitro experiments clearly show a dose-dependent and PPARδ receptor–mediated effect of PPARδ ligands, in vivo the attenuation of neointima formation was more effective with low-dose GW0742-Me–coated stents. We cannot exclude that the inverse dose-dependent effect of PPARδ ligand (GW0742-Me)–coated stents on neointima formation comes from PPARδ receptor–independent modes of action such as activation or inhibition of other nuclear receptors. Thus Nandhikonda et al[37] previously reported that GW0742 exhibits characteristics of a pan nuclear receptor antagonist at high concentrations. In addition, differences in neointima formation could represent local toxicity caused by high-dose GW0742-Me–coated stents. Moreover, in our study, stents were not examined beyond 42 days, thus precluding assessment of possibly different long-term effect of high-dose and low-dose GW0742-Me–coated stents on neointima formation.

In-stent restenosis and bypass graft failure are characterized by excessive VSMC proliferation, leading to luminal narrowing. However, data on the role of PPARδ in modulating cell proliferation are controversial, as both increased and decreased cell proliferation rates by synthetic PPARδ ligands have been reported previously.[19,38] Whereas Lim et al[19] reported that adenovirus-mediated overexpression of PPARδ suppresses PDGF-induced VSMC proliferation, Zhang et al[39] found that overexpression of PPARδ in VSMCs increases postconfluent cell proliferation. In addition, Lim et al used L-165041, the first synthetic compound that not only activates PPARδ, but also triggers PPARγ activation at high doses.[40] As the role of the nuclear receptor PPARδ in mediating the opposite growth modulatory effects of PPARδ ligands on various cell types has not clearly been defined, we analyzed the effect of GW0742 on both normal and PPARδ-depleted VSMCs. Our data indicate that the PPARδ ligand GW0742 inhibits proliferation and migration of VSMCs in vitro in a PPARδ receptor–dependent manner. Given the increased energy requirements for cell proliferation and chemotaxis, we examined the effect of the synthetic PPARδ agonist GW0742 on glycolysis and mitochondrial respiration using extracellular flux analysis. Consistent with previously published studies,[11] our data demonstrate that PDGF stimulation enhances glycolysis in VSMCs. We found that under both acute and chronic treatment conditions, GW0742 inhibits PDGF-induced augmentation of glycolysis. In addition, GW0742 treatment significantly attenuates the maximal respiratory capacity and the reserve respiratory capacity and increases the mitochondrial proton leak respiration. The observed effect of GW0742 on PDGF-induced glycolysis and mitochondrial respiration impairs the ability of VSMCs to provide the increased energy demands required for growth factor–stimulated proliferation and migration of VSMCs. PPARδ activation is known to regulate many genes involved in fatty acid and glucose utilization.[41] However, data about the effect of PPARδ ligands on glucose metabolism are controversial, as both impaired and increased glucose utilization has been reported.[42,43] Our data show that GW0742 treatment strongly induces pyruvate dehydrogenase kinase isozyme 4 in VSMCs. Pyruvate dehydrogenase kinase isozyme 4 phosphorylates and inactivates pyruvate dehydrogenase, which inhibits the utilization of pyruvate for acetyl-CoA synthesis and thus blocks glucose oxidation. In addition, we found that the expression of GLUT1, the predominant isoform of glucose transporter proteins in VSMCs,[24] was significantly reduced in response to GW0742 treatment.

The signaling pathways that link changes in VSMC energy metabolism and function are poorly understood. Recently, AMPK emerged as important regulator of metabolic processes and VSMC migration and proliferation.[44] Our data demonstrate that GW0742 treatment of VSMCs induces AMPK phosphorylation of the catalytic α domain at threonine 172. AMPK is a key metabolic sensor that is phosphorylated in response to cellular energy deprivation and stress[45] and acts to restore energy homeostasis by switching off ATP-consuming processes and switching on catabolic pathways that generate ATP. However, the relationship of AMPK in PPARδ-mediated inhibition of cell proliferation is complex. As AMPK activation in skeletal muscle was previously found to be PPARδ independent,[43] the observed induction of AMPK phosphorylation in VSMCs after GW0742 treatment is likely either because of the change in cellular energy metabolism or mediated directly via heme oxygenase-1 (Figure IV in the online-only Data Supplement). In accordance, Kim et al[46] recently observed that heme oxygenase-1 induces activation of AMPK in VSMCs.

The inflammatory response of VSMCs plays an important role in neointima formation after PCI. Our data demonstrate that PPARδ ligands inhibit tumor necrosis factor-α–induced expression of IL-6, MCP-1, and VCAM by inducing Bcl-6 binding to the corresponding inflammatory gene promoter sequence. Early studies indicate that PPARγ is not required for the anti-inflammatory effect of its ligands.[47] However, by use of primary cultures of VSMCs from wild-type and PPARδ$^{-/-}$ mice, we demonstrate that PPARδ ligands inhibit inflammatory gene expression in a receptor-dependent manner. Taken together, GW0742 affects crucial biological VSMC functions, including proliferation and gene expression, which is compatible with beneficial outcome in experimental restenosis.

The interaction of platelets with the surface of DES plays an important role in both in-stent restenosis and stent thrombosis. Thrombocyte adhesion and aggregation is mediated by a variety of surface glycoproteins such as GP IIb/IIIa, GP VI, or the GP Ib–IX–V complex.[48] On Upon activation, GP IIb/IIIa undergoes a conformational change, and additional intraplatelet pools of GP IIb/IIIa are released that increase the surface density. In addition, von Willebrand factor plays an important role in platelet adhesion at the site of endothelial injury, as it mediates platelet–subendothelium interaction by linking the platelet receptor GP Ib–IX–X to the extracellular matrix.[49] To date, no stent coating with an antithrombotic effect has been developed. Strikingly, we found that GW0742-Me coating effectively prevents human thrombocyte deposition to the stents surface and thrombocyte activation in vitro. As determined by flow cytometry, both platelet surface receptor GP IIb/IIIa surface density and activation (PAC-1 binding) increased after perfusion of vehicle-coated stents, whereas no change was observed with GW0742-Me–coated stents. In addition, perfusion of vehicle-coated stents increased the thrombin–antithrombin III values, indicating the thrombin generation of adhering activated platelets, which leads to the activation of the plasmatic coagulation. The density of GP Ib receptor per platelet was significantly reduced in the vehicle-coated stent group, which reflects a higher activation in the closed-loop system.[50] Furthermore, PPARδ ligand GW0742 dose-dependently inhibited ristocetin-induced human thrombocyte aggregation in vitro, whereas no effect was observed on collagen-induced platelet aggregation at a concentration of 5 μg/mL. Both ristocetin and collagen induce platelet aggregation via common pathways such as activation of phospholipase C (PLC). However, as ristocetin forms a complex with von Willebrand factor that facilitates binding to the GP Ib–IX–V complex, the specific inhibition of ristocetin-induced platelet aggregation by GW0742 could be attributed to an inhibition or dissociation of the von Willebrand factor—GP Ib–IX–V complex.

In contrast to our observation, Ali et al[29] reported in 2006 that PPARδ ligands (L-165041; GW0742) inhibit human platelet activation induced by various stimuli such as collagen, thrombin, and ADP. However, in this study, measurements were performed in whole-blood and higher concentrations of both the agonists and the PPARδ ligand GW0742 were used, which might explain the different results. Thus, it was recently reported that nitrite inhibits P-selectin expression on the platelet membrane and GP IIb/IIIa activation in response to ADP, collagen, and thrombin stimulation in the presence of erythrocytes, and this inhibition was promoted by increasing hematocrit and deoxygenation of erythrocytes (what takes place during storage), suggesting that NO produced by the reaction of nitrite with deoxyhemoglobin was responsible for this inhibitory effect.[51] Whereas a previous study reported that the ability of PPARδ agonist GW501516 to inhibit ADP-induced platelet aggregation was similar in PPARδ$^{-/-}$ and PPARδ$^{+/+}$ mouse thrombocytes,[52] our data demonstrate that GW0742 mediated inhibition of thrombocyte aggregation is receptor dependent, as the effect was abolished in PPARδ$^{-/-}$ platelets. In summary, differences between previous reports and our results might be attributed to a variety of different factors, including different specificities of PPARδ agonists for other PPAR isoforms, different potencies of various PPARδ compounds, different in vitro conditions (whole-blood versus platelet-rich plasma), or use of different PPARδ knockout mouse models.

Recent studies indicate that a rapid re-endothelialization of the stented area is associated with a lower risk of inflammation and subsequent thrombus formation.[53] A major concern with currently used DES is impaired re-endothelialization because of the drug.[54] Endothelial regrowth after stenting depends on both migration from intact neighboring coronary segments, and attraction and adhesion of circulating endothelial progenitor cells. Previous studies have shown that sirolimus and paclitaxel inhibit proliferation and migration of ECs in vitro,[55,56] thereby potentially impairing re-endothelialization. Data on the role of PPARδ in ECs are controversial, as both proproliferative and antiproliferative effects have been reported.[33,34] Our data demonstrate that GW0742 induces proliferation and VEGF-induced migration of cultured ECs. In addition, adhesion and spreading, essential processes for EC migration, were accelerated in GW0742-treated ECs. However, in our rabbit model of experimental atherosclerosis, no difference in re-endothelialization was evident with the use of GW0742-coated stents compared with vehicle-coated stents as endothelial regrowth was already almost complete at day 14 (Figure V in the online-only Data Supplement). Although animal models of stenting probably predict human responses as the stages of healing are remarkably similar, previous studies have shown that endothelial regrowth is significantly more rapid in the rabbit model than in the humans, where re-endothelialization is only complete by 3 to 4 months after bare-metal stent implantation or may even not fully endothelialize several years after implantation.[6,57] We did not clearly define the underlying mechanism responsible for the contrary effect of PPARδ activation by synthetic ligands on proliferation/migration of VSMCs and ECs. However, we can speculate that the different effect of PPARδ on proliferation of VSMCs and EC comes from cell-type–specific expression levels of coactivators and corepressors, differences in post-translational modifications and proteosomal degradation of PPARδ.

In conclusion, our data demonstrate that PPARδ ligand–coated stents lead to significant inhibition of in-stent neointima formation compared with vehicle-coated stents. We attribute this effect to an inhibition of VSMC proliferation and inflammatory gene expression and potentially an inhibition of thrombocyte activation and a proproliferative and promigratory effect on ECs. Thus, PPARδ ligand–coated stents might be a promising strategy to address the problems of in-stent restenosis and late-stent thrombosis. Further preclinical studies and clinical trials are needed to test this hypothesis.

Acknowledgments

We thank Beatrice Leip and Saskia Mueller for excellent technical assistance.

Sources of Funding

The study was supported by a Research Grant from Philipp Morris USA Inc. and a Twinning Research Grant from the Max-Delbrueck-Centrum for Molecular Medicine.

Disclosures

None.

References

1. Roger VL, Go AS, Lloyd-Jones DM, et al.; American Heart Association Statistics Committee and Stroke Statistics Subcommittee. Executive summary: heart disease and stroke statistics–2012 update: a report from the American Heart Association. *Circulation*. 2012;125:188–197. doi: 10.1161/CIR.0b013e3182456d46.
2. Thom T, Haase N, Rosamond W, et al.; American Heart Association Statistics Committee and Stroke Statistics Subcommittee. Heart disease and stroke statistics–2006 update: a report from the American Heart Association Statistics Committee and Stroke Statistics Subcommittee. *Circulation*. 2006;113:e85–151. doi: 10.1161/CIRCULATIONAHA.105.171600.
3. Inoue T, Node K. Molecular basis of restenosis and novel issues of drug-eluting stents. *Circ J*. 2009;73:615–621.
4. Babinska A, Markell MS, Salifu MO, Akoad M, Ehrlich YH, Kornecki E. Enhancement of human platelet aggregation and secretion induced by rapamycin. *Nephrol Dial Transplant*. 1998;13:3153–3159.
5. Granada JF, Alviar CL, Wallace-Bradley D, Osteen M, Dave B, Tellez A, Win HK, Kleiman NS, Kaluza GL, Lev EI. Patterns of activation and deposition of platelets exposed to the polymeric surface of the paclitaxel eluting stent. *J Thromb Thrombolysis*. 2010;29:60–69. doi: 10.1007/s11239-009-0348-9.
6. Joner M, Finn AV, Farb A, Mont EK, Kolodgie FD, Ladich E, Kutys R, Skorija K, Gold HK, Virmani R. Pathology of drug-eluting stents in humans: delayed healing and late thrombotic risk. *J Am Coll Cardiol*. 2006;48:193–202. doi: 10.1016/j.jacc.2006.03.042.
7. Mack CP. Signaling mechanisms that regulate smooth muscle cell differentiation. *Arterioscler Thromb Vasc Biol*. 2011;31:1495–1505. doi: 10.1161/ATVBAHA.110.221135.
8. Libby P, Schwartz D, Brogi E, Tanaka H, Clinton SK. A cascade model for restenosis. A special case of atherosclerosis progression. *Circulation*. 1992;86(6 suppl):III47–III52.
9. Yang X, Thomas DP, Zhang X, Culver BW, Alexander BM, Murdoch WJ, Rao MN, Tulis DA, Ren J, Sreejayan N. Curcumin inhibits platelet-derived growth factor-stimulated vascular smooth muscle cell function and injury-induced neointima formation. *Arterioscler Thromb Vasc Biol*. 2006;26:85–90. doi: 10.1161/01.ATV.0000191635.00744.b6.
10. Vander Heiden MG, Cantley LC, Thompson CB. Understanding the Warburg effect: the metabolic requirements of cell proliferation. *Science*. 2009;324:1029–1033. doi: 10.1126/science.1160809.

11. Perez J, Hill BG, Benavides GA, Dranka BP, Darley-Usmar VM. Role of cellular bioenergetics in smooth muscle cell proliferation induced by platelet-derived growth factor. *Biochem J*. 2010;428:255–267. doi: 10.1042/BJ20100090.
12. Barish GD, Narkar VA, Evans RM. PPAR delta: a dagger in the heart of the metabolic syndrome. *J Clin Invest*. 2006;116:590–597. doi: 10.1172/JCI27955.
13. Bishop-Bailey D, Bystrom J. Emerging roles of peroxisome proliferator-activated receptor-beta/delta in inflammation. *Pharmacol Ther*. 2009;124:141–150. doi: 10.1016/j.pharmthera.2009.06.011.
14. Bojic LA, Huff MW. Peroxisome proliferator-activated receptor δ: a multifaceted metabolic player. *Curr Opin Lipidol*. 2013;24:171–177. doi: 10.1097/MOL.0b013e32835cc949.
15. Bays HE, Schwartz S, Littlejohn T III, Kerzner B, Krauss RM, Karpf DB, Choi YJ, Wang X, Naim S, Roberts BK. MBX-8025, a novel peroxisome proliferator receptor-delta agonist: lipid and other metabolic effects in dyslipidemic overweight patients treated with and without atorvastatin. *J Clin Endocrinol Metab*. 2011;96:2889–2897. doi: 10.1210/jc.2011-1061.
16. Olson EJ, Pearce GL, Jones NP, Sprecher DL. Lipid effects of peroxisome proliferator-activated receptor-δ agonist GW501516 in subjects with low high-density lipoprotein cholesterol: characteristics of metabolic syndrome. *Arterioscler Thromb Vasc Biol*. 2012;32:2289–2294. doi: 10.1161/ATVBAHA.112.247890.
17. Marmur JD, Poon M, Rossikhina M, Taubman MB. Induction of PDGF-responsive genes in vascular smooth muscle. Implications for the early response to vessel injury. *Circulation*. 1992;86(6 suppl):III53–III60.
18. Doran AC, Meller N, McNamara CA. Role of smooth muscle cells in the initiation and early progression of atherosclerosis. *Arterioscler Thromb Vasc Biol*. 2008;28:812–819. doi: 10.1161/ATVBAHA.107.159327.
19. Lim HJ, Lee S, Park JH, Lee KS, Choi HE, Chung KS, Lee HH, Park HY. PPAR delta agonist L-165041 inhibits rat vascular smooth muscle cell proliferation and migration via inhibition of cell cycle. *Atherosclerosis*. 2009;202:446–454. doi: 10.1016/j.atherosclerosis.2008.05.023.
20. Burdick AD, Bility MT, Girroir EE, Billin AN, Willson TM, Gonzalez FJ, Peters JM. Ligand activation of peroxisome proliferator-activated receptor-beta/delta(PPARbeta/delta) inhibits cell growth of human N/TERT-1 keratinocytes. *Cell Signal*. 2007;19:1163–1171. doi: 10.1016/j.cellsig.2006.12.007.
21. Romanowska M, al Yacoub N, Seidel H, Donandt S, Gerken H, Phillip S, Haritonova N, Artuc M, Schweiger S, Sterry W, Foerster J. PPARdelta enhances keratinocyte proliferation in psoriasis and induces heparin-binding EGF-like growth factor. *J Invest Dermatol*. 2008;128:110–124. doi: 10.1038/sj.jid.5700943.
22. Han S, Ritzenthaler JD, Zheng Y, Roman J. PPARbeta/delta agonist stimulates human lung carcinoma cell growth through inhibition of PTEN expression: the involvement of PI3K and NF-kappaB signals. *Am J Physiol Lung Cell Mol Physiol*. 2008;294:L1238–L1249. doi: 10.1152/ajplung.00017.2008.
23. Rubin LJ, Magliola L, Feng X, Jones AW, Hale CC. Metabolic activation of AMP kinase in vascular smooth muscle. *J Appl Physiol (1985)*. 2005;98:296–306. doi: 10.1152/japplphysiol.00075.2004.
24. Klip A, Tsakiridis T, Marette A, Ortiz PA. Regulation of expression of glucose transporters by glucose: a review of studies *in vivo* and in cell cultures. *FASEB J*. 1994;8:43–53.
25. Schober A. Chemokines in vascular dysfunction and remodeling. *Arterioscler Thromb Vasc Biol*. 2008;28:1950–1959. doi: 10.1161/ATVBAHA.107.161224.
26. Lee CH, Chawla A, Urbiztondo N, Liao D, Boisvert WA, Evans RM, Curtiss LK. Transcriptional repression of atherogenic inflammation: modulation by PPARdelta. *Science*. 2003;302:453–457. doi: 10.1126/science.1087344.
27. McNicol A, Israels SJ. Beyond hemostasis: the role of platelets in inflammation, malignancy and infection. *Cardiovasc Hematol Disord Drug Targets*. 2008;8:99–117.
28. Akbiyik F, Ray DM, Gettings KF, Blumberg N, Francis CW, Phipps RP. Human bone marrow megakaryocytes and platelets express PPARgamma, and PPARgamma agonists blunt platelet release of CD40 ligand and thromboxanes. *Blood*. 2004;104:1361–1368. doi: 10.1182/blood-2004-03-0926.
29. Ali FY, Davidson SJ, Moraes LA, Traves SL, Paul-Clark M, Bishop-Bailey D, Warner TD, Mitchell JA. Role of nuclear receptor signaling in platelets: antithrombotic effects of PPARbeta. *FASEB J*. 2006;20:326–328. doi: 10.1096/fj.05-4395fje.
30. Ray DM, Spinelli SL, Pollock SJ, Murant TI, O'Brien JJ, Blumberg N, Francis CW, Taubman MB, Phipps RP. Peroxisome proliferator-activated receptor gamma and retinoid X receptor transcription factors are released from activated human platelets and shed in microparticles. *Thromb Haemost*. 2008;99:86–95. doi: 10.1160/TH07-05-0328.
31. Mrowietz C, Franke RP, Seyfert UT, Park JW, Jung F. Haemocompatibility of polymer-coated stainless steel stents as compared to uncoated stents. *Clin Hemorheol Microcirc*. 2005;32:89–103.
32. Liou JY, Lee S, Ghelani D, Matijevic-Aleksic N, Wu KK. Protection of endothelial survival by peroxisome proliferator-activated receptor-delta mediated 14-3-3 upregulation. *Arterioscler Thromb Vasc Biol*. 2006;26:1481–1487. doi: 10.1161/01.ATV.0000223875.14120.93.
33. Piqueras L, Reynolds AR, Hodivala-Dilke KM, Alfranca A, Redondo JM, Hatae T, Tanabe T, Warner TD, Bishop-Bailey D. Activation of PPARbeta/delta induces endothelial cell proliferation and angiogenesis. *Arterioscler Thromb Vasc Biol*. 2007;27:63–69. doi: 10.1161/01.ATV.0000250972.83623.61.
34. Park JH, Lee KS, Lim HJ, Kim H, Kwak HJ, Park HY. The PPARδ ligand L-165041 inhibits VEGF-induced angiogenesis, but the antiangiogenic effect is not related to PPARδ. *J Cell Biochem*. 2012;113:1947–1954. doi: 10.1002/jcb.24063.
35. Guagliumi G, Ikejima H, Sirbu V, Bezerra H, Musumeci G, Lortkipanidze N, Fiocca L, Tahara S, Vassileva A, Matiashvili A, Valsecchi O, Costa M. Impact of drug release kinetics on vascular response to different zotarolimus-eluting stents implanted in patients with long coronary stenoses: the LongOCT study (Optical Coherence Tomography in Long Lesions). *JACC Cardiovasc Interv*. 2011;4:778–785. doi: 10.1016/j.jcin.2011.04.007.
36. Palmaz JC TF, Schatz RA, Alvarado R, Rees C, Garcia FS. Early endothelialization of balloon-expandable stents: experimental observations. *J Intervent Radiol*. 1988;3:119–124.
37. Nandhikonda P, Yasgar A, Baranowski AM, et al. Peroxisome proliferation-activated receptor δ agonist GW0742 interacts weakly with multiple nuclear receptors, including the vitamin D receptor. *Biochemistry*. 2013;52:4193–4203. doi: 10.1021/bi400321p.
38. Kostadinova R, Montagner A, Gouranton E, Fleury S, Guillou H, Dombrowicz D, Desreumaux P, Wahli W. GW501516-activated PPARβ/δ promotes liver fibrosis via p38-JNK MAPK-induced hepatic stellate cell proliferation. *Cell Biosci*. 2012;2:34. doi: 10.1186/2045-3701-2-34.
39. Zhang J, Fu M, Zhu X, Xiao Y, Mou Y, Zheng H, Akinbami MA, Wang Q, Chen YE. Peroxisome proliferator-activated receptor delta is up-regulated during vascular lesion formation and promotes post-confluent cell proliferation in vascular smooth muscle cells. *J Biol Chem*. 2002;277:11505–11512. doi: 10.1074/jbc.M110580200.
40. Wurch T, Junquero D, Delhon A, Pauwels J. Pharmacological analysis of wild-type alpha, gamma and delta subtypes of the human peroxisome proliferator-activated receptor. *Naunyn Schmiedebergs Arch Pharmacol*. 2002;365:133–140. doi: 10.1007/s00210-001-0504-z.
41. Nakamura MT, Yudell BE, Loor JJ. Regulation of energy metabolism by long-chain fatty acids. *Prog Lipid Res*. 2014;53:124–144. doi: 10.1016/j.plipres.2013.12.001.
42. Brunmair B, Staniek K, Dörig J, Szöcs Z, Stadlbauer K, Marian V, Gras F, Anderwald C, Nohl H, Waldhäusl W, Fürnsinn C. Activation of PPAR-delta in isolated rat skeletal muscle switches fuel preference from glucose to fatty acids. *Diabetologia*. 2006;49:2713–2722. doi: 10.1007/s00125-006-0357-6.
43. Krämer DK, Al-Khalili L, Guigas B, Leng Y, Garcia-Roves PM, Krook A. Role of AMP kinase and PPARdelta in the regulation of lipid and glucose metabolism in human skeletal muscle. *J Biol Chem*. 2007;282:19313–19320. doi: 10.1074/jbc.M702329200.
44. Stone JD, Narine A, Shaver PR, Fox JC, Vuncannon JR, Tulis DA. AMP-activated protein kinase inhibits vascular smooth muscle cell proliferation and migration and vascular remodeling following injury. *Am J Physiol Heart Circ Physiol*. 2013;304:H369–H381. doi: 10.1152/ajpheart.00446.2012.
45. Hardie DG, Ross FA, Hawley SA. AMPK: a nutrient and energy sensor that maintains energy homeostasis. *Nat Rev Mol Cell Biol*. 2012;13:251–262. doi: 10.1038/nrm3311.
46. Kim JE, Sung JY, Woo CH, Kang YJ, Lee KY, Kim HS, Kwun WH, Choi HC. Cilostazol inhibits vascular smooth muscle cell proliferation and reactive oxygen species production through activation of AMP-activated protein kinase induced by heme oxygenase-1. *Korean J Physiol Pharmacol*. 2011;15:203–210. doi: 10.4196/kjpp.2011.15.4.203.
47. Chawla A, Barak Y, Nagy L, Liao D, Tontonoz P, Evans RM. PPAR-gamma dependent and independent effects on macrophage-gene

expression in lipid metabolism and inflammation. *Nat Med*. 2001;7:48–52. doi: 10.1038/83336.
48. Rivera J, Lozano ML, Navarro-Núñez L, Vicente V. Platelet receptors and signaling in the dynamics of thrombus formation. *Haematologica*. 2009;94:700–711. doi: 10.3324/haematol.2008.003178.
49. Savage B, Cattaneo M, Ruggeri ZM. Mechanisms of platelet aggregation. *Curr Opin Hematol*. 2001;8:270–276.
50. van Zanten GH, Heijnen HF, Wu Y, Schut-Hese KM, Slootweg PJ, de Groot PG, Sixma JJ, Nieuwland R. A fifty percent reduction of platelet surface glycoprotein Ib does not affect platelet adhesion under flow conditions. *Blood*. 1998;91:2353–2359.
51. Akrawinthawong K, Park JW, Piknova B, Sibmooh N, Fucharoen S, Schechter AN. A flow cytometric analysis of the inhibition of platelet reactivity due to nitrite reduction by deoxygenated erythrocytes. *PLoS One*. 2014;9:e92435. doi: 10.1371/journal.pone.0092435.
52. Ali FY, Hall MG, Desvergne B, Warner TD, Mitchell JA. PPARbeta/delta agonists modulate platelet function via a mechanism involving PPAR receptors and specific association/repression of PKCalpha–brief report. *Arterioscler Thromb Vasc Biol*. 2009;29:1871–1873. doi: 10.1161/ATVBAHA.109.193367.
53. Youn YJ, Lee JW, Ahn SG, et al. Study design and rationale of "a multicenter, open-labeled, randomized controlled trial comparing three 2nd-generation drug-eluting stents in real-world practice" (CHOICE trial). *Am Heart J*. 2013;166:224–229. doi: 10.1016/j.ahj.2013.04.014.
54. Webster MW, Ormiston JA. Drug-eluting stents and late stent thrombosis. *Lancet*. 2007;370:914–915. doi: 10.1016/S0140-6736(07)61424-X.
55. Wessely R, Blaich B, Belaiba RS, Merl S, Görlach A, Kastrati A, Schömig A. Comparative characterization of cellular and molecular anti-restenotic profiles of paclitaxel and sirolimus. Implications for local drug delivery. *Thromb Haemost*. 2007;97:1003–1012.
56. Kakade S, Mani G. A comparative study of the effects of vitamin C, sirolimus, and paclitaxel on the growth of endothelial and smooth muscle cells for cardiovascular medical device applications. *Drug Des Devel Ther*. 2013;7:529–544. doi: 10.2147/DDDT.S45162.
57. Virmani R, Kolodgie FD, Farb A, Lafont A. Drug eluting stents: are human and animal studies comparable? *Heart*. 2003;89:133–138.

Highlights

- Peroxisome proliferator–activated receptor-delta (PPARδ) ligand–coated stents significantly inhibit strut-associated neointima compared with bare-metal stents in a rabbit model of experimental atherosclerosis.
- PPARδ ligands inhibit proliferation and migration and inflammatory gene expression of vascular smooth muscle cells.
- PPARδ ligands inhibit thrombocyte activation and aggregation.
- PPARδ ligands induce proliferation and migration of endothelial cells.
- Pharmacological PPARδ activation is a promising novel strategy to address drawbacks of currently used drug-eluting coronary stents.

Arteriosclerosis, Thrombosis, and Vascular Biology

JOURNAL OF THE AMERICAN HEART ASSOCIATION

Activation of Peroxisome Proliferator–Activated Receptor-δ as Novel Therapeutic Strategy to Prevent In-Stent Restenosis and Stent Thrombosis

Jarkko Hytönen, Olli Leppaenen, Jan Hinrich Braesen, Wolf-Hagen Schunck, Dominik Mueller, Friedrich Jung, Christoph Mrowietz, Martin Jastroch, Michael von Bergwelt-Baildon, Kai Kappert, Arnd Heuser, Jörg-Detlef Drenckhahn, Burkert Pieske, Ludwig Thierfelder, Seppo Ylä-Herttuala and Florian Blaschke

Arterioscler Thromb Vasc Biol. published online June 9, 2016;
Arteriosclerosis, Thrombosis, and Vascular Biology is published by the American Heart Association, 7272 Greenville Avenue, Dallas, TX 75231

Print ISSN: 1079-5642. Online ISSN: 1524-4636

SUPPLEMENTAL MATERIAL

MATERIAL AND METHODS

Materials

Antibodies were purchased from the following suppliers: p-AMPK alpha and total AMPK alpha from Cell Signaling, Bcl-6 from Santa Cruz Biotechnology, PPARδ (sc-1987) and PECAM-1 (sc-1506) from Santa Cruz Biotechnology, anti-rabbit macrophage (clone RAM11) and Ki67 (clone Ki-67) from Dako, smooth muscle actin (clone HHF35) and CD68 from Thermo Scientific™ Lab Vision. The anti-topoisomerase II (clone KiS1) was kindly provided by Prof. Wolfram Klapper (University Clinic Kiel, Germany). The Bcl-6 expression plasmid was kindly provided from Ari Melnick (Weill Cornell Medical College, NY, USA) and the HO-1 promoter constructs were generously provided by Mark Perella (Brigham and Women's Hospital, Boston, USA). PPARδ knockout and wildtype mice were kindly provided by Frank J. Gonzalez (National Cancer Institute, Rockville, USA). GW0742 was provided by Dr. Timothy M. Willson (GlaxoSmithKline Inc, Durham, NC).

Human Coronary Samples

Stented coronary artery segments were obtained during autopsy at the Institute for Pathology of the University Hospital of Hamburg. A total of 21 samples were collected 3 hours to 3 years after stenting from 6 patients. In addition, 3 samples from a nonstented coronary artery were analyzed.(1) The protocol was approved by the ethics committee of the University Hospital of Hamburg.

Rabbit Model of Experimental Atherosclerosis

The study was approved by the University of Kuopio Research Animal Ethics Committee and conforms to National Institutes of health guidelines. A rabbit model of experimental atherosclerosis was used as previously described.(2, 3) Briefly, 46 New Zealand white rabbits (3.0 to 4.0 kg; Lidkoeping Kaninfarm, Sweden) were fed an atherogenic diet consisting of 1% cholesterol and 6% peanut oil for 5 weeks. After one week of high cholesterol diet, a 3-French Fogarty embolectomy catheter was advanced into the right iliac artery and aorta and withdrawn with the balloon inflated. After aortic denudation, the animals were maintained on an atherogenic diet for additional 4 weeks before stent implantation. Subsequent, the diet was switched to a low cholesterol diet (containing 0.025% cholesterol). Blood samples were drawn at the time of aortic denudation, at the end of the atherogenic diet, before stent deployment and at euthanasia for determination of the differential blood count and measurement of various serum parameters. Animals were kept on a 12/12 hour-dark cycle with ad libitum access to food and water.

Stent Coating

Polymer-free stents (YUKON®ChoiceDES, 20 x 3.5 mm, Translumina GmbH) were coated with the methylester conjugated PPARδ ligand GW0742 (GW0742-Me). GW0742-Me was prepared treating GW0742 (100 mg/ 6 ml ethanol) with an excess of ethereal diazomethane until the yellow color of diazomethane persisted. After 20 min at room temperature, the remaining diazomethane and solvent were removed under reduced pressure. This reaction resulted in a complete conversion of GW0742 to its methylester as proved by reversed-phase HPLC. For stent coating, the cartridge was placed into the stent coating device and a 1 ml drug reservoir containing the dissolved drug in a predefined volume was connected to the cartridge. The coating process was initialized by the advancement of the drug into a mobile, positionable ring containing three jet units, which allow for uniform delivery of the drug onto the stent surface. For low-dose coating, the spray solution contained 4.5 mg GW0742-Me/ml ethanol. High-dose coating was achieved by spraying the stents twice with 7.5 mg GW0742-Me/ml ethanol. Subsequently to spray coating, the stent surface was dried by removing the ethanol with

pressured air. Any potentially remaining ethanol vaporizes after storage for one or two days according to the stent manufacturer Translumina®. To estimate the amount of GW0742-Me bound to the stent surface, three stents of each the low- and high-dose group were used and the compound was eluted with 5 and 20 ml of ethanol, respectively. The eluted GW0742-Me was determined spectrophotometrically using its characteristic absorption maxima at 232 and 318 nm and corresponding linear calibration curves with the authentic standard compound. Based on these measurements, 151.2 ± 15.4 µg and 445.3 ± 61.2 µg GW0742 were bound to the stent surface after low- and high-dose coating, respectively. Covering of the stent surface with the GW0742-Me coating was analyzed using electron scanning microcopy (Zeiss DSM 962, Germany).

Stent Placement and Tissue Harvest

After induction of general anesthesia and heparinization (150 IU/kg), a 5-French arterial introducing sheath was placed into the left carotid artery. PPARδ ligand (GW0742-Me) or vehicle (ethanol) coated stents were deployed in an infrarenal aortic segment free of side branches and dilated by inflation to their nominal pressure (9 to 11 atm, 30 sec balloon inflation). After stent implantation, an angiography was performed to document vessel patency and exclude a dissection. All animals received aspirin from day 3 and clopidogrel from day 1 before the stent implantation until euthanasia. Fourteen days and forty-two days after stent deployment animals were euthanized and stented sites were excised for mRNA, immunohistochemical, and morphometric analyses. In addition, a 3-mm arterial segment proximal to the stents was processed to evaluate for edge effects.

Immunhistochemistry and Morphometric Analyses

The stented rabbit aortas and human coronary arteries were collected, fixed en bloc in 4% neutral buffered formalin, and dehydrated with a graded series of alcohol before embedding in methylmethacrylate (MMA) as previously described.(1) For immunohistochemistry, sections were deplastinized and stained with antibodies recognizing macrophages (CD68 or Ram11), HHF35 to detect smooth muscle cells, CD31 or PECAM-1 to quantify re-endothelialization, and to KiS1 or Ki67 to assess proliferation. Deplastination was carried out in 2-methoxyethyl acetate for 45 to 90 min. For toluidine blue staining sections without deplastination were used. Quantitative measurements of the neointima and media were made on cross-sectioned rabbit aortas stained with toluidine blue. Cell proliferation was assessed by counting Ki67-positive cells, macrophage and smooth muscle content was determined using computer assisted morphometry (Zeiss Axiovision). Paraffin embedding and immunohistochemistry of rat carotid arteries were performed as described previously.(4) Controls for immunostaining included stainings in which the primary antibody was omitted.

Cell Culture

Human umbilical vein endothelial cells (HUVECs) were commercially obtained (Lonza, USA) and expanded in EBM-2 supplemented with the EGM™-2 Bulletkit™ according to the manufacturer instructions for 3 to 5 passages. Mouse primary aortic VSMCs (mVSMCs) were prepared from aortas of 8- to 12-week old PPARδ$^{+/+}$ or PPARδ$^{-/-}$ mice as described.(5) Rat aortic VSMCs (rVSMCs) were isolated as previously described.(6) Both mVSMCs and rVSMCs were maintained and passaged in DMEM supplemented with 10% fetal bovine serum (FBS), L-glutamine (200 mmol/L) and 1% penicillin/streptomycin. In all experiments, VSMCs of passage four to ten were subjected to G_0/G_1 phase synchronization by starvation for at least 24 hours in medium containing 0.2% FBS. Cells were pretreated for 24 hours with the indicated doses of PPARδ ligand (GW0742) or vehicle (DMSO) prior to stimulation with PDGF-BB (25 ng/ml) or TNFα (10 ng/ml). Cell viability was measured using a commercially available MTT assay.

GW0742 exhibited no effect on cell viability (data not shown). All experiments were repeated at least three times with different cell preparations.

Reverse Transcription and Quantitative Real-time Polymerase Chain Reaction
Total RNA isolation was performed using the RNeasy MINI Kit (QUIAGEN), and RNA was reverse transcribed with random hexamers using the TaqMan Reverse Transcription Reagent Kit (Applied Biosystems) according to the manufacturer's instructions. Transcript levels of target genes were assessed using an iQ5 real-time PCR Detection System (Bio-Rad). Each sample was analyzed in triplicate and mRNA levels of glyceraldehydes-3-phosphate dehydrogenase (GAPDH) were quantified and used as housekeeping gene in human and murine cells, respectively. Primer and probes in the experiments were obtained from Applied Biosystems.

Protein Assays
Western blots were performed as previously described.(4) Briefly, cells were harvested at the indicated time points and sonicated in solubilization buffer (Cell Signaling). Whole cell lysates were cleared by centrifugation, protein concentrations were determined by Lowry assay (Bio-Rad) and equal amount of proteins were resolved by SDS-page.

Cell Proliferation Assays
Mouse and rat VSMCs were serum-deprived for at least 24 hours and incubated with the PPARδ ligand GW0742 as indicated. After stimulation with PDGF-BB (25 ng/ml), cell proliferation was assessed by cell counting using a hematocytometer or an ATP assay, as previously described.(4) HUVECs were seeded and grown for 48 hours in the absence or presence of sirolimus (10 nM), tacrolimus (20 μM) or GW0742 (1 μM).

Two-dimensional Chemotaxis Assay
Directional cell migration was examined using the μ-Slides from Ibidi (Ibidi, Germany) according to the manufacturer's instructions. Briefly, cells were seeded into the center of a μ-Slide chamber and incubated for 2 hours until cells were attached. After cells were washed with medium to remove non-adherent cells PDGF-BB (25 ng/ml) or VEGF (50 ng/ml) was added as chemoattractant for rVSMCs or HUVECs respectively. Cell movement was monitored by live-cell imaging. Cell tracking analysis was performed with ImageJ software (National Institutes of Health, Bethesda, USA).

Cell Spreading Assay
The xCELLigence system (Roche Applied Science) was used to analyze the effect of PPARδ ligand GW0742 on cell adhesion and spreading according to the manufacturer's instructions. Briefly, HUVECs pretreated with 3 μM GW0742 for 18 hours were seeded onto a 96-well-microtiter xCELLigence assay plate (E-plate; 10.000 cells per well) and placed on the Real-time xCELLigence Cell Analyzer platform to continuously measure impedance changes across microelectrodes integrated on the bottom of the E-plates. Impedance changes occur if cell attach to E-plates or change their size, shape and numbers.

Chromatin Immunoprecipitation Assay
Chromatin immunoprecipitation (ChIP) assays were performed using a ChIP assay kit from Upstate as previously described.(7) Briefly, cells were treated with 10 μM GW0742 and stimulated with TNFα (10 ng/ml) as indicated. Cells were crosslinked with 2 mmol/L disuccinimidyl glutarate for 45 minutes before crosslinking for 15 minutes with 1% formaldehyde. This 2-step crosslinking method has been shown to be more efficient than the conventional single formaldehyde crosslinking procedure.(8) After lysis, cells were sonicated and chromatin

fragments were immunoprecipitated with an antibody directed against Bcl-6 overnight at 4˚C. Rabbit IgG was used as a negative control. DNA fragments were purified from chromatin using the QIAquick PCR Purification Kit (QIAGEN) according to the instructions of the manufacturer. The final DNA extractions were amplified by PCR using specific primers for the IL-6, MCP-1 and VCAM promoter. An equal volume of nonprecipitated (input) genomic DNA was amplified as positive control. The PCR products were resolved on 2% agarose gels and visualized using ethidium bromide.

Measurement of Cellular Bioenergetic Function Using the XF-24 Extracellular Flux Analyzer

The XF24 Extracellular Flux Analyzer (Seahorse Bioscience; Billerica) was used to analyze the effect of PPARδ ligand GW0742 on both acute and chronic PDGF-treatment induced glycolytic flux and mitochondrial respiration in rVSMCs. The oxygen consumption rate (OCR) and the extracellular acidification rate (ECAR) were determined following treatment with or without GW0742 and/or PDGF stimulation. Cell culture medium was changed prior to the bioenergetic measurements to serum-free unbuffered (without sodium bicarbonate) DMEM medium supplemented with 2 mM L-glutamine, 5.5 mM D-glucose and 1 mM sodium pyruvate. Basal OCRs and ECARs were measured, followed by the sequential injection of 2 μg/ml oligomycin and 1 uM FCCP (carbonyl cyanide p-trifluoromethoxy-phenylhydrazone) and 2.5 uM of each rotenone/antimycin A. Total cell number, determined after each experiment, was determined by DAPI staining and light microscopy and used to normalize glycolytic rates and mitochondrial oxidation.

Transient Transfections and Luciferase Assay

Transient transfections of rVSMCs were performed in triplicate using FuGENE 6 reagent (Roche). Luciferase activity was assayed with the Dual-Luciferase Reporter Assay System (Promega) according to manufacturer's instructions. Transfection efficiency was adjusted by normalizing firefly luciferase activities to renilla luciferase activities generated by co-transfecting pRL-TK (Promega).

Platelet-rich Plasma

Blood was collected in citrated tubes from apparently healthy subjects who did not take any drugs known to interfere with platelet aggregation for at least 14 days. Human platelet-rich plasma was prepared by centrifugation of citrate-anticoagulated blood at 120 g for 15 min. Mouse platelet-rich plasma was prepared by collecting blood from the vena cava inferior of 12 week old female PPAR$\delta^{+/+}$ and PPAR$\delta^{-/-}$ mice, followed by centrifugation at 90 g for 12 min.

Stent Perfusion *in Vitro*

PPARδ ligand (GW0742-Me) and vehicle (EtOH) coated stents were implanted into a closed-loop system and perfused with platelet rich plasma. Measurements were taken immediately after the filling of the perfusion system and after 1, 11 and 21 circulations. Thrombocyte aggregation and activation was determined as described previously.(9) The thrombin-antithrombin III-complex was measured using the ELISA Enzygnost TAT (Behringwerke, Germany).

Flow cytometry

Formaldehyde fixed thrombocytes were processed for flow cytometric analysis, which was carried out on a Cytomics FC 500, equipped with the CXP software (Beckman Coulter®, Krefeld, Germany). A calibration of the device was performed prior to all analyses including the Immuno-Brite™ standard kit (Beckman Coulter®, Krefeld, Germany) and FluoroSpheres calibration beads (Dako, Hamburg,Germany). Mean thrombocyte receptor densities were calculated from the mean equivalent fluorochrome amounts using the FluoroSpheres calibration beads (Dako,

Hamburg, Germany) as standards. The ratio of the fluorochrome molecules to the number of antibody molecules (F/P ratio) was calculated batch-specific, according to the information of the supplier. To identify thrombocytes, samples were stained for the GPIb/IX thrombocyte membrane glycoprotein (anti-CD42b-PE (Clone SZ2), Immunotech, Beckman Coulter; anti-CD42a-FITC (Clone Beb1), Becton Dickinson Bioscience). The lysosomal membrane associated glycoprotein 3 (anti-CD63-FITC (Clone CLBGran/12), Immunotech, Beckman Coulter) and the activated GPIIbIIIa receptor (anti-PAC-1-FITC, Becton Dickinson Bioscience) were analyzed, as markers for the activation of thrombocytes.

Platelet Aggregation *in Vitro*

Platelet aggregation was carried out according to the turbidimetric method of Born in a four-channel light transmission aggregometer (APACT-4004; Haemochrom Diagnostica, Germany).(10) Platelet-rich plasma was pre-incubated with the PPARδ ligand GW0742 before stimulation of aggregation by addition of either adenosine diphosphat (ADP, 10 μM), collagen (5 μg/ml) or ristocetin (0.75 mg/ml). To measure aggregation on mouse platelets, fibrinogen had to be added, which serves as a ligand to cross-link platelets. Thus, mouse platelet-rich plasma was diluted in human platelet poor plasma. The PPARδ ligand GW0742 was solved in ethanol. Ethanol had no effect on platelet aggregation (data not shown).

Statistical Analysis

All data are expressed as mean ± standard error of mean (SEM). The data displayed normal variance. Intergroup differences were appropriately assessed by either unpaired two-tailed Student´s t-test (for comparison of two groups) or one-way analysis of variance (ANOVA) with Bonferroni´s post-hoc test (for comparison of more than two groups). The significance threshold was set at $P \leq 0.05$. Statistical analysis were performed using GraphPad PRISM v6 (GraphPad Software®).

SUPPLEMENTAL LITERATURE

1. Brasen JH, Kivela A, Roser K, Rissanen TT, Niemi M, Luft FC, Donath K, Yla-Herttuala S. Angiogenesis, vascular endothelial growth factor and platelet-derived growth factor-BB expression, iron deposition, and oxidation-specific epitopes in stented human coronary arteries. Arterioscler Thromb Vasc Biol. 2001;21(11):1720-6.
2. Joner M, Farb A, Cheng Q, Finn AV, Acampado E, Burke AP, Skorija K, Creighton W, Kolodgie FD, Gold HK, Virmani R. Pioglitazone inhibits in-stent restenosis in atherosclerotic rabbits by targeting transforming growth factor-beta and MCP-1. Arterioscler Thromb Vasc Biol. 2007;27(1):182-9.
3. Hiltunen MO, Laitinen M, Turunen MP et al. Intravascular adenovirus-mediated VEGF-C gene transfer reduces neointima formation in balloon-denuded rabbit aorta. Circulation. 2000;102(18):2262-8.
4. Blaschke F, Leppanen O, Takata Y, Caglayan E, Liu J, Fishbein MC, Kappert K, Nakayama KI, Collins AR, Fleck E, Hsueh WA, Law RE, Bruemmer D. Liver X receptor agonists suppress vascular smooth muscle cell proliferation and inhibit neointima formation in balloon-injured rat carotid arteries. Circ Res. 2004;95(12):e110-23.
5. Nomiyama T, Nakamachi T, Gizard F, Heywood EB, Jones KL, Ohkura N, Kawamori R, Conneely OM, Bruemmer D. The NR4A orphan nuclear receptor NOR1 is induced by platelet-derived growth factor and mediates vascular smooth muscle cell proliferation. J Biol Chem. 2006;281(44):33467-76.
6. Blaschke F, Stawowy P, Kappert K, Goetze S, Kintscher U, Wollert-Wulf B, Fleck E, Graf K. Angiotensin II-augmented migration of VSMCs towards PDGF-BB involves Pyk2 and ERK 1/2 activation. Basic Res Cardiol. 2002;97(4):334-42.

7. Blaschke F, Takata Y, Caglayan E, Collins A, Tontonoz P, Hsueh WA, Tangirala RK. A nuclear receptor corepressor-dependent pathway mediates suppression of cytokine-induced C-reactive protein gene expression by liver X receptor. Circ Res. 2006;99(12):e88-99.
8. Nowak DE, Tian B, Brasier AR. Two-step cross-linking method for identification of NF-kappaB gene network by chromatin immunoprecipitation. Biotechniques. 2005;39(5):715-25.
9. Jung F, Braune S, Lendlein A. Haemocompatibility testing of biomaterials using human platelets. Clin Hemorheol Microcirc. 2013;53(1-2):97-115.
10. Born GV, Cross MJ. The Aggregation of Blood Platelets. J Physiol. 1963;168:178-95.

SUPPLEMENTAL MATERIAL

SUPPLEMENTAL RESULTS

Release Kinetic of PPARδ Ligand Coated Stents

For determination of pharmacological release kinetics, PPARδ (GW0742) coated stents (n=3) were deployed *ex vivo* and submersed in 1 ml PBS at 37°C. Samples harvested at distinct time points were subjected to high-performance liquid chromatography (HPLC)-based analysis. Time dependent HPLC-based analysis of GW0742 elution from coated stents indicated that most of the ligand was released within the first 15 min (Supplemental Figure IA, *left*). Although an optimal release kinetic has not been determined so far for any compound used on drug eluting stents, a release kinetic within a few hours is not satisfactory.

To achieve a longer release kinetic we modified the synthetic PPARδ ligand GW0742. GW0742 has a single carboxyl group within its structure which is suitable for forming ester compounds. Diazomethane was utilized to produce methylesters of GW0742 (GW0742-Me) and thus to modify the solubility (Supplemental Figure IIA). After methylation, the release of PPARδ ligand from the stent *in vitro* was extended to more than 2 weeks (Supplemental Figure IA, *right*). The surface of a GW0742-Me-coated stent is depicted in Supplemental Figure IB. Importantly, both GW0742 and GW0742-Me exert similar biological effects, as determined by quantification of the PPARδ target gene Adfp (adipose differentiation related protein) expression in J774 cells in response to ligand treatment (Supplemental Figure IIB). In addition, cotransfection of PPARδ followed by GW0742 and GW0742-Me stimulation induced PPRE reporter activity in a comparable manner (4.67-fold at 10 μM GW0742 and 5.56-fold at 10 μM GW0742-Me versus unstimulated cells; $P<0.05$; Supplemental Figure IIC).

To determine the pharmacokinetics of PPARδ ligand-coated stents *in vivo*, rabbits (n=4) were stented in the abdominal aorta and euthanized on day three after stenting. Blood samples, drawn 15 min after intervention and subsequently at 6, 12, 24 and 48 hours after stenting, revealed perceptible PPARδ ligand blood levels with a maximum at 6 h after stent deployment (Supplemental Figure IC, *left*). PPARδ ligand levels in the vascular wall were determined 3 days after stent placement. Measurement of the concentrations of both GW0742-Me and GW0742 in serum and vessel wall using the Triple-Quadrupole Tandem Mass Spectrometer Agilent 6410 combined with the Agilent 1200 HPLC System revealed a rapid conversion of GW0742-Me to GW0742 (Supplemental Figure IC, *right*).

PPARδ Induces Transcription of Heme Oxygenase-1 in VSMCs

Previous studies have shown that heme oxygenase-1 (HO-1), an inducible stress protein known for its cytoprotective functions, exerts antiproliferative effects in VSMCs.(11, 12) To determine the effect of synthetic PPARδ ligands on HO-1 expression, quiescent rVSMCs were incubated with GW0742 as indicated. As shown in Figure IVA, PPARδ agonist treatment markedly increased HO-1 mRNA (2.23-fold induction versus unstimulated cells; $P<0.05$) and protein expression. To address the role of PPARδ in regulating HO-1 expression, serum-deprived $PPAR\delta^{+/+}$ and $PPAR\delta^{-/-}$ mVSMCs were used. Stimulation of PPARδ wildtype mVSMCs with GW0742 induced HO-1 mRNA expression (2.85-fold induction versus unstimulated cells; $P<0.05$), whereas no effect was observed in PPARδ knockout cells (Figure IVB). Taken together, these results indicate that PPARδ ligands induce HO-1 gene transcription in a receptor-dependent manner. To identify the HO-1 promoter elements that mediate the response to ligand-activated PPARδ, we used a series of 5'-deletion constructs. As depicted in Figure IVC, the inducibility by GW0742 was lost in the -66HO1-Luc and -35HO1-Luc constructs.

As previous studies reported a growth-inhibitory effect of HO-1,(11, 12) we therefore conclude that the enhanced HO-1 expression in response to PPARδ ligand treatment contributes to its anti-proliferative effect.

Supplemental Figure Legends

Suppl. Figure I

(**A**) Pharmacokinetics of GW0742 and GW0742-Me coated stents *in vitro* (n = 3 per group). Cumulative GW0742 (*left*) and GW0742-Me (*right*) release profile in PBS solution at 37˚C. (**B**) GW0742-Me-coated surface of an unexpanded stent (scale bar: 100 μM). (**C**) Kinetics of drug release from GW0742-Me coated stents under *in vivo* conditions (n = 4 per group). Release into the blood stream was characterized by measuring the serum levels of both GW0742-Me and the deconjugated GW0742 since the methylester is rapidly cleaved, presumably by esterases present in the plasma (*left*). Right panel shows the tissue levels of GW0742 (GW) and GW0742-Me (GW-Me) in the vascular wall 3 days after stent implantation.

Suppl. Figure II

(**A**) The chemical structure of PPARδ ligand GW0742 (GW) and methylester conjugated PPARδ ligand GW0742-Me (GW-Me). (**B**) Serum-deprived J774A.1 cells were treated with 10 μM GW0742 or GW0742-Me for 24 hours. Cells were the harvested and analyzed for Adfp mRNA expression by quantitative real-time PCR. (**C**) rVSMCs were transiently transfected with a PPARδ overexpression plasmid and a PPRE-Luc reporter driven by three PPRE binding sites. At 24 hours after transfection, cells were stimulated with 10 μM GW0742 or GW0742-Me. Firefly luciferase activity was analyzed and normalized to renilla luciferase activity obtained by co-transfecting pRL-TK. Data are presented as fold induction±SEM over unstimulated control. *P<0.05 vs unstimulated cells, one-way ANOVA with post hoc correction (Bonferroni).

Suppl. Figure III

(**A**) Study layout of stent placement in a rabbit model of experimental atherosclerosis. (**B**) Representative photographs of rabbit aortas after denudation and additional 4 weeks of atherogenic diet illustrating the development of atherosclerotic lesions. Serial sections were stained with trichrom-elastin, for macrophages (Mac-2) and for endothelial cells (CD31). (**C**) Representative angiograms before stent deployment, during balloon inflation and after stent placement.

Suppl. Figure IV

PPARδ activation induces heme oxygenase-1 (HO-1) mRNA and protein expression in G_1-arrested rVSMCs (**A**) and PPARδ$^{+/+}$ mVSMCs (**B**). Rat VSMCs and PPARδ$^{+/+}$ (PPARδ WT) and PPARδ$^{-/-}$ (PPARδ KO) mVSMCs were serum-starved for 24 hours followed by stimulation with GW0742 (GW) as indicated. HO-1 mRNA and protein expression was analyzed by quantitative real-time PCR (normalized to GAPDH mRNA expression) or Western blotting, normalized to smooth muscle actin (SMA). (**C**) Regulation of the HO-1 promoter by PPARδ. Rat VSMCs were transiently transfected with HO-1 promoter constructs, followed by stimulation with GW0742 (10 μM). Luciferase activity was assayed 24 hours after PPARδ ligand treatment. Data are expressed as fold induction±SEM over unstimulated control (Con). *P<0.05 vs. unstimulated cells, one-way ANOVA with *post hoc* correction (Bonferroni). Western blots are representative of 3 independent experiments.

Suppl. Figure V

Re-endothelialization of vehicle (ethanol) and PPARδ ligand (GW0742-Me) coated stents 14 days after deployment in rabbit atheromatous arteries (n = 8 per group). (A) Representative arterial sections stained with an antibody against PECAM-1 (platelet endothelial cell adhesion molecule-1) to visualize endothelial cells. (B) Quantification of luminal endothelial cell coverage. Results are presented as mean±SEM, Student´s t-test.

Suppl. Figure VI
Proposed mechanism of PPARδ ligand coated stents in suppressing neointima formation and stent thrombosis.

Suppl. Table I
Metabolic parameters (**A**) and differential blood count (**B**) of rabbits 42 days after deployment of vehicle (EtOH) and GW0742-Me coated stents. Values are expressed as mean±SEM, one-way ANOVA with post hoc correction (Bonferroni).

SUPPLEMENTAL LITERATURE

1. Brasen JH, Kivela A, Roser K, Rissanen TT, Niemi M, Luft FC, Donath K, Yla-Herttuala S. Angiogenesis, vascular endothelial growth factor and platelet-derived growth factor-BB expression, iron deposition, and oxidation-specific epitopes in stented human coronary arteries. Arterioscler Thromb Vasc Biol. 2001;21(11):1720-6.
2. Joner M, Farb A, Cheng Q, Finn AV, Acampado E, Burke AP, Skorija K, Creighton W, Kolodgie FD, Gold HK, Virmani R. Pioglitazone inhibits in-stent restenosis in atherosclerotic rabbits by targeting transforming growth factor-beta and MCP-1. Arterioscler Thromb Vasc Biol. 2007;27(1):182-9.
3. Hiltunen MO, Laitinen M, Turunen MP et al. Intravascular adenovirus-mediated VEGF-C gene transfer reduces neointima formation in balloon-denuded rabbit aorta. Circulation. 2000;102(18):2262-8.
4. Blaschke F, Leppanen O, Takata Y, Caglayan E, Liu J, Fishbein MC, Kappert K, Nakayama KI, Collins AR, Fleck E, Hsueh WA, Law RE, Bruemmer D. Liver X receptor agonists suppress vascular smooth muscle cell proliferation and inhibit neointima formation in balloon-injured rat carotid arteries. Circ Res. 2004;95(12):e110-23.
5. Nomiyama T, Nakamachi T, Gizard F, Heywood EB, Jones KL, Ohkura N, Kawamori R, Conneely OM, Bruemmer D. The NR4A orphan nuclear receptor NOR1 is induced by platelet-derived growth factor and mediates vascular smooth muscle cell proliferation. J Biol Chem. 2006;281(44):33467-76.
6. Blaschke F, Stawowy P, Kappert K, Goetze S, Kintscher U, Wollert-Wulf B, Fleck E, Graf K. Angiotensin II-augmented migration of VSMCs towards PDGF-BB involves Pyk2 and ERK 1/2 activation. Basic Res Cardiol. 2002;97(4):334-42.
7. Blaschke F, Takata Y, Caglayan E, Collins A, Tontonoz P, Hsueh WA, Tangirala RK. A nuclear receptor corepressor-dependent pathway mediates suppression of cytokine-induced C-reactive protein gene expression by liver X receptor. Circ Res. 2006;99(12):e88-99.
8. Nowak DE, Tian B, Brasier AR. Two-step cross-linking method for identification of NF-kappaB gene network by chromatin immunoprecipitation. Biotechniques. 2005;39(5):715-25.
9. Jung F, Braune S, Lendlein A. Haemocompatibility testing of biomaterials using human platelets. Clin Hemorheol Microcirc. 2013;53(1-2):97-115.
10. Born GV, Cross MJ. The Aggregation of Blood Platelets. J Physiol. 1963;168:178-95.
11. Sheng-Long C, Yan-Xin W, Yi-Yi H, Ming F, Jian-Gui H, Yi-Li C, Wen-Jing X, Hong M. AVE0991, a Nonpeptide Compound, Attenuates Angiotensin II-Induced Vascular Smooth Muscle Cell Proliferation via Induction of Heme Oxygenase-1 and Downregulation of p-38 MAPK Phosphorylation. Int J Hypertens. 2012;2012:958298.
12. Pae HO, Jeong GS, Jeong SO, Kim HS, Kim SA, Kim YC, Yoo SJ, Kim HD, Chung HT. Roles of heme oxygenase-1 in curcumin-induced growth inhibition in rat smooth muscle cells. Exp Mol Med. 2007;39(3):267-77.

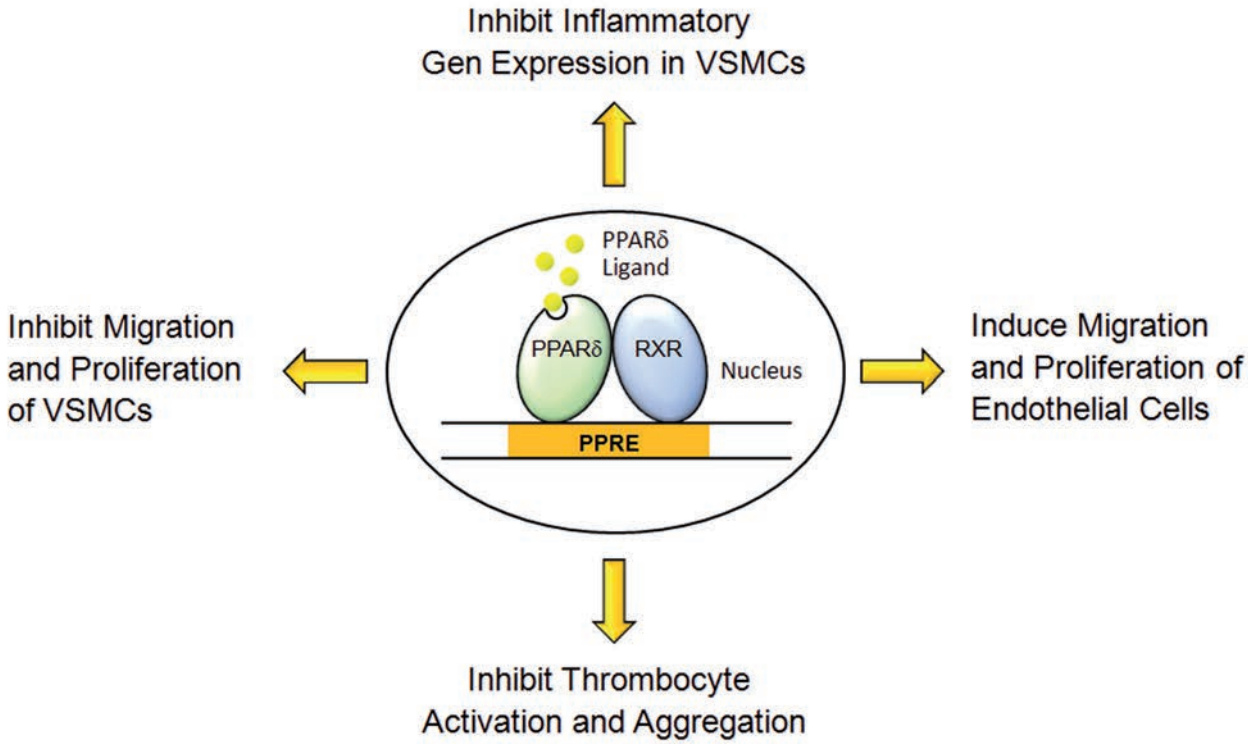
Inhibit Inflammatory
Gen Expression in VSMCs
PPARδ
Ligand
PPARδ
RXR
Nucleus
PPRE
Inhibit Migration
and Proliferation
of VSMCs
Induce Migration
and Proliferation of
Endothelial Cells
Inhibit Thrombocyte
Activation and Aggregation

Figure 6